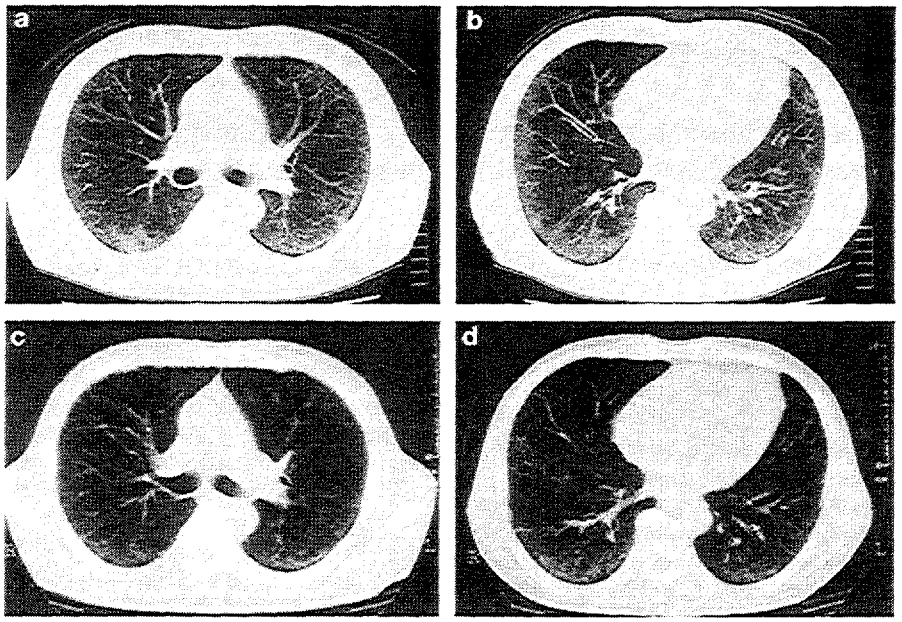

Figure 1 Chest CT performed before initiation and after cessation of imatinib mesylate. CT scans obtained at the level of bronchus intermedius (a) and lung bases (b) revealed reticular shadow and ground-glass opacities at subpleural area in both lung. CT scans obtained 18 days after discontinuation of imatinib mesylate at the level of bronchus intermedius (c) and lung bases (d) revealed that reticular shadow and ground-glass opacities almost disappeared.

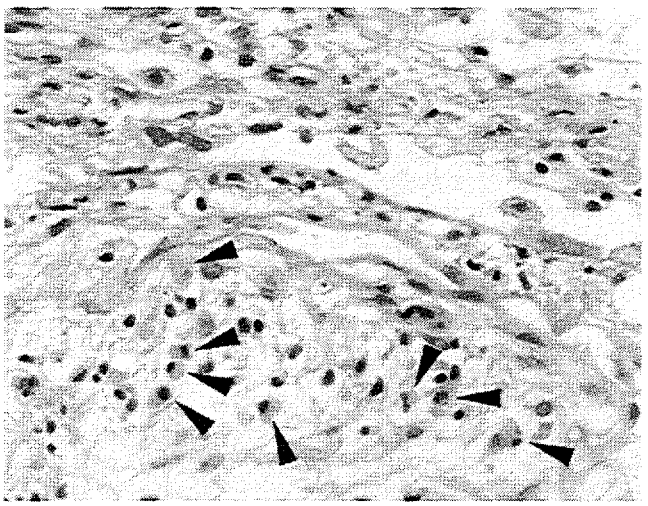

Figure 2 Pathological findings of transbrochial lung biopsy. Alveolar structures were destroyed in most of the microscopic field in the TBLB specimen. Prominent infiltration of eosinophilic leukocytes (indicated by arrows) was observed in loose fibrous tissue. These findings are compatible with drug-induced interstitial pneumonia. (H–E stain, ×400).

lacked pathologic corroboration.[4] Recently, Rosado *et al*[5] also reported a case of imatinib-induced interstitial pneumonia diagnosed by TBLB, but whose pathological findings were compatible with the nonspecific interstitial pneumonia without eosinophilic infiltration. The above data, taken together with our observations, suggest that imatinib-induced interstitial pneumonia may be heterogeneous and some of them may be likely to involve an immunoallergic mechanism. So far, the frequency of interstitial pneumonia related to imatinib appears to be relatively low and the underlying mechanism is still unclear; however, we must pay close attention to this adverse event.

T Yokoyama[1]
K Miyazawa[1]
E Kurakawa[1]
A Nagate[1]
T Shimamoto[1]
K Iwaya[2]
S Akata[3]
M Aoshima[1]
H Serizawa[2]
K Ohyashiki[1]

[1]*First Department of Internal Medicine, Tokyo Medical University, Japan;*
[2]*Division of Surgical Pathology, Tokyo Medical University, Japan; and*
[3]*Department of Radiology, Tokyo Medical University, Japan*

References

1 O'Brien SG, Guilhot F, Larson RA, Gathmann I, Baccarani M, Cervantes F *et al.* IRIS investigators: imatinib compared with interferon low-dose cytarabine for newly diagnosed chronic-phase chronic myeloid leukemia. *N Engl J Med* 2003; **348**: 994–1004.
2 Hehlmann R. Current CML therapy: progress and dilemma. *Leukemia* 2003; **17**: 1010–1012.
3 Kantarjian H, Sawyers C, Hochhaus A, Guilhot F, Schiffer C, Gambacorti-Passerini C *et al.* International STI571 CML Study Group: hematologic and cytogenetic responses to imatinib mesylate in chronic myelogenous leukemia. *N Engl J Med* 2002; **346**: 645–652.
4 Bergeron A, Bergot E, Vilela G, Ades L, Devergie A, Esperou H *et al.* Hypersensitivity pneumonitis related to imatinib mesylate. *J Clin Oncol* 2002; **20**: 4271–4272.
5 Rosado MF, Donna E, Ahn YS. Challenging problems in advanced malignancy: case 3. Imatinib mesylate-induced interstitial pneumonitis. *J Clin Oncol* 2003; **21**: 3171–3173.

Stromal cell–derived factor-1α/CXCL12–induced chemotaxis of T cells involves activation of the RasGAP-associated docking protein p62Dok-1

Seiichi Okabe, Seiji Fukuda, Young-June Kim, Masaru Niki, Louis M. Pelus, Kazuma Ohyashiki, Pier Paolo Pandolfi, and Hal E. Broxmeyer

Events mediating stromal cell–derived factor-1 (SDF-1α/CXCL12) chemotaxis of lymphocytes are not completely known. We evaluated intracellular signaling through RasGAP-associated protein p62Dok-1 (downstream of tyrosine kinase [Dok-1]) and associated proteins. SDF-1α/CXCL12 stimulated Dok-1 tyrosine phosphorylation and association with RasGAP, adaptor protein p46Nck, and Crk-L in Jurkat T cells. The phosphorylation of Dok-1 was blocked by pretreatment of cells with the src kinase inhibitor PP2. Src kinase family member Lck was implicated. SDF-1α/CXCL12 did not phosphorylate Dok-1 in J.CaM1.6 cells, a Jurkat derivative not expressing Lck, but did phosphorylate Dok-1 in J.CaM1.6 cells expressing Lck. SDF-1α/CXCL12 induced the tyrosine phosphorylation of Pyk2 and the association of Pyk2 with zeta chain–associated protein-70 kilodaltons (Zap-70) and Vav. SDF-1α/CXCL12 enhanced the association of RasGAP with Pyk2. CXCR4–expressing NIH3T3 and Baf3 cells transfected with full-length Dok-1 cDNA were suppressed in their responses to SDF-1α/CXCL12–induced chemotaxis; mitogen-activated protein (MAP) kinase activity was also decreased. Chemotaxis to SDF-1/CXCL12 was significantly enhanced in Dok-1$^{-/-}$ CD4$^+$ and CD8$^+$ splenic T cells. These results implicate Dok-1, Nck, Crk-L, and Src kinases—especially Lck, Pyk2, Zap-70, Vav, and Ras-GAP—in intracellular signaling by SDF-1α/CXCL12, and they suggest that Dok-1 plays an important role in SDF-1α/CXCL12–induced chemotaxis in T cells. (Blood. 2005;105:474-480)

Introduction

Chemokines play a central role in lymphocyte trafficking and homing. The chemokine stromal cell–derived factor-1α (SDF-1α/CXCL12) binds to CXC chemokine receptor 4 (CXCR4).[1,2] CXCR4 is a 7-transmembrane surface structure linked to G proteins.[3] CXCR4 is expressed on a number of cell types, including T cells, hematopoietic stem cells, and progenitor cells. SDF-1α/CXCL12 is a highly efficient chemoattractant for T lymphocytes and other cells. Targeted disruption of SDF-1α/CXCL12 or CXCR4 is lethal in mice and is associated with the absence of lymphoid and myeloid hematopoiesis in the fetal bone marrow.[4,5]

The p120RasGAP-associated p62 protein Dok-1 (downstream of tyrosine kinase) was originally defined as a tyrosine-phosphorylated 62-kDa protein that coimmunoprecipitated with p21Ras GTPase-activating protein (RasGAP).[6] Dok-1 is a docking protein purified from v-Abl or BCR-Abl–transformed hematopoietic cells. It consists of pleckstrin homology (PH) and phosphotyrosine binding (PTB) domains in the amino-terminal and the tyrosine phosphorylation site.[7] Dok-1 is tyrosine phosphorylated by several cytokines, such as kit-ligand, platelet-derived growth factor (PDGF), and vascular endothelial growth factor (VEGF), and couples with the cytoplasmic protein tyrosine kinase (PTK).[8,9] Dok-1 is considered to be a downstream target of PTKs and to play a negative role in various signaling pathways.[10]

RasGAP is an essential component of Ras-activated signaling pathways. RasGAP has GTPase stimulating activity in the carboxy-terminus and has 2 src homology domains (SH2) and 1 SH3 domain in the amino-terminal region. RasGAP down-regulates Ras activity, converting the activate form of RasGTP to the inactive form, RasGDP, and it plays a role in cell growth and differentiation.[11,12]

Proline-rich tyrosine kinase 2 (Pyk2), also known as cellular adhesion kinase β (CAKβ), related adhesion focal tyrosine kinase (RAFTK), and calcium-dependent tyrosine kinase (CADTK) are predominantly expressed in cells derived from hematopoietic lineages and in the central nervous system.[13-16] Pyk2 is one of the signaling mediators critical for signaling through G protein–coupled receptors, is activated by signals that elevate intracellular calcium concentrations, and is required for activation of mitogen-activated protein kinase (MAPK) signaling. Pyk2 is tyrosine phosphorylated after T-cell receptor (TCR) stimulation.[17,18]

The aims of our study were to evaluate intracellular effects mediating the chemotaxis induced by SDF-1α/CXCL12 and to determine whether this intracellular signaling pathway involved Dok-1, RasGAP, or Pyk2. Our results suggest that Dok-1, RasGAP, and Pyk2 are involved in SDF-1α/CXCL12 signaling.

Materials and methods

Reagents and antibody

Recombinant human SDF-1α/CXCL12, antiphosphotyrosine monoclonal antibody (mAb; 4G10) and anti–Crk-L mAb were purchased from Upstate

From the Department of Microbiology/Immunology and the Walther Oncology Center, Indiana University School of Medicine, Indianapolis, and the Walther Cancer Institute, Indianapolis, IN; the Cancer Biology and Genetics Program and the Department of Pathology, Memorial Sloan Kettering Cancer Center, New York, NY; and the First Department of Internal Medicine, Tokyo Medical University, Japan.

Submitted March 5, 2004; accepted September 1, 2004. Prepublished online as *Blood* First Edition Paper, September 2, 2004; DOI 10.1182/blood-2004-03-0843.

Supported by US Public Health Service National Institutes of Health grants RO1 HL67384 and RO1 DK53674 (H.E.B.) and RO1 HL69669 (L.M.P.).

Reprints: Hal E. Broxmeyer, Walther Oncology Center, Indiana University School of Medicine, 950 W Walnut St, Indianapolis, IN 46202; e-mail: hbroxmey@iupui.edu.

The publication costs of this article were defrayed in part by page charge payment. Therefore, and solely to indicate this fact, this article is hereby marked "advertisement" in accordance with 18 U.S.C. section 1734.

Biotechnology (Lake Placid, NY). Rabbit anti–Dok-1 antibody (Ab), agarose-conjugated goat anti–Dok-1 Ab, anti-RasGAP mAb, anti-Vav Ab, phopho-ERK1 Ab, and protein A/G agarose were obtained from Santa Cruz Biotechnology (Santa Cruz, CA). Rabbit anti–Dok-1 Ab was purchased from Prosci Incorporated (Poway, CA). Antiphosphotyrosine mAb (PY20), anti-Pyk2 mAb, and anti-Nck mAb, and anti–Zap-70 mAb were obtained from Transduction Laboratories (Lexington, KY). Src kinase inhibitor PP2 was obtained from Calbiochem-Novabiochem (San Diego, CA). Anti-CXCR4 mAb was from R&D Systems (Minneapolis, MN). Other reagents were from Sigma (St Louis, MO).

Construction of plasmid

The plasmid encoding mouse dok-1 was kindly provided by Dr Y. Yamanashi (Tokyo University, Japan). The complementary DNA (cDNA) encoding full-length dok-1 was amplified by polymerase chain reaction and was cloned into a mammalian GFP-expressing vector, GFP Fusion TOPO TA Expression Kits (Invitrogen, Carlsbad, CA), or a retroviral vector (pQCXIR; Clontech, Palo Alto, CA) at the *NotI*/*PswI* site.

Cell culture, transfection, and infection

Human leukemic T-cell line Jurkat, Lck-deficient T-cell line J.CaM1.6, and J.CaM1.6 cells engineered to express Lck were maintained in RPMI 1640 medium supplemented with 10% heat-inactivated fetal bovine serum (FBS) with 1% penicillin/streptomycin in a humidified incubator at 37°C. Murine fibroblast NIH3T3 cells expressing human CXCR4 and CD4 were maintained in Dulbecco modified Eagle minimal medium (DMEM) supplemented with 2 mM L-glutamine and 1% penicillin/streptomycin. Transfections were performed using LipofectAMINE 2000 (Invitrogen) according to the manufacturer's protocol. After transfection, cells were sorted using flow cytometry and were used for chemotaxis assay. For retroviral production, Phoenix-echo cells were transfected with empty vector alone or with full-length dok-1 using LipofectAMINE 2000 (Invitrogen). Supernatant was collected 24 hours and 48 hours after transfection. NIH3T3 cells were infected using supernatant and were analyzed by Western blot. Murine IL-3–dependent cell line Baf-3 and Dok-1–transfected Baf-3 Dok cells were cultured with 10% fetal calf serum (FCS) RPMI 1640 with 0.1 ng/mL murine interleukin-3 (IL-3). Lck cDNA expressing J.CaM/Lck cells were kind gifts from A. Weiss (University of California, San Francisco) and were cultured with 10% FCS RPMI 1640.

Immunoprecipitation and Western blot analysis

Jurkat, J.CaM1.6, and NIH3T3 cells were factor starved overnight and treated with 100 ng/mL SDF-1α/CXCL12, a predetermined optimal concentration, at the indicated times and were washed once with ice-cold phosphate-buffered saline (PBS). Cells were lysed in lysis buffer containing 20 mM Tris-HCl, pH 8.0, 137 mM NaCl, 10% glycerol, 1 mM phenylmethylsulfonyl fluoride (PMSF), 10 μM ethylenediaminetetraacetic acid (EDTA), 10 μg/mL leupeptin, 100 mM sodium fluoride, 2 mM sodium orthovanadate, and 1% NP-40 for 20 minutes on ice. Lysates were centrifuged at 12 000 rpm (10 000 × g) for 20 minutes at 4°C. The protein content of lysates was determined with a protein assay kit (Bio-Rad Laboratories, Hercules, CA). Equivalent amounts of protein in cell lysates were boiled with 2 × SDS (sodium dodecyl sulfate) sample buffer for 5 minutes. For immunoprecipitation, cell lysates were incubated at 4°C overnight with the indicated precipitating antibody. Immunoprecipitates were collected using 40 μL protein A/G–agarose for 2 hours at 4°C. After 4 washings in lysis buffer, immunocomplexes were eluted and boiled for 5 minutes in 2 × sample buffer. Proteins or immunocomplexes were loaded onto polyacrylamide gels (BioWhittaker, Walkersville, MD) and then were transferred to polyvinylidene difluoride (PVDF) membranes (Millipore, Bedford, MA). The membranes were blocked by 3% skim milk, PBS-Tween 20 (PBST) or 1% bovine serum albumin (BSA) PBST and probed with the indicated primary antibody at appropriate dilutions for 2 hours at room temperature (RT) or overnight at 4°C. Blots were probed with secondary antibody–conjugated horseradish peroxidase, and were developed using the enhanced chemiluminescence (ECL; Amersham Phamacia Biotech, Bucks, United Kingdom) system with ECL film according to the manufacturer's specification.

Chemotaxis assay

Chemotaxis assays for Jurkat, J.CaM1.6, and NIH3T3 cells were performed with 48-well microchemotaxis chambers with 8-μm pore size polycarbonate filters (PVP free; NeuroProbe, Gaithersburg, MD). Filters were soaked overnight in 0.1% wt/vol gelatin solution (Sigma). The chemotaxis medium (0.2% BSA in DMEM with and without 100 ng/mL SDF-1α/CXCL12) was placed in the lower chamber, and 50 μL cell suspension (1.6×10^5 cells/mL) in chemotaxis medium (without SDF-1α/CXCL12) was placed in the upper wells. After incubation of the apparatus at 37°C for 3 to 4 hours in humidified air with 5% CO_2, filters were removed, fixed, and stained with the use of DiffQuik staining kit (Dade Behring, Newark, DE). Cells were counted in 3 high-power fields (HPFs; 400 ×). Results were expressed as the mean number of migrating cells in 1 HPF.

Transmigration assay of splenic T cells

Splenic T cells from $Dok^{-/-}$ and control mice[19] were isolated by negative selection using the pan T-cell isolation kit (Miltenyi Biotech, Auburn, CA), which depletes cells expressing B220, Gr-1, and Ter119. The purity of T cells was evaluated by staining CD4 and CD8 and was greater than 95%. The chemotaxis assay to SDF1α/CXCL12 in the face of positive, negative, and zero gradient was performed as described.[20] After a 4-hour migration assay, input cells and cells that migrated to the bottom chamber were enumerated and stained with fluorescein isothiocyanate (FITC)–conjugated anti-CD4 and phycoerythrin (PE)–conjugated anti-CD8 antibodies (BD Biosciences, San Diego, CA) to determine the migration of T-cell subsets by flow cytometry. Migration index was calculated by the number of cells migrated divided by the background migration without SDF1α/CXCL12. Expression of CXCR4 was determined by staining the isolated T cells with biotinylated antimouse CXCR4 mAb (clone 2B11/CXCR4; BD Biosciences) with or without anti-CD4 and anti-CD8 Abs, followed by cytochrome-conjugated streptavidin staining.

Flow cytometric analysis

NIH3T3 cells were detached by incubation with 10 mM EDTA in DMEM for 10 minutes, transferred to tubes, and sedimented (10 000 rpm, 1 minute [7000 × g]). Cells were stimulated with 100 ng/mL SDF-1α/CXCL12 at 37°C for the indicated times, washed once in ice-cold PBS, and fixed using the Cytofix/Cytoperm kit (BD PharMingen, San Diego, CA) or 1% paraformaldehyde PBS. Cells were incubated with phospho-Erk1 Ab for 1 hour and then incubated with phycoerythrin (PE)–conjugated secondary antibody. MAPK activities were monitored by flow cytometric analysis, and data obtained from 5 independent measurements were evaluated with the Student *t* test. To evaluate cell surface CXCR4, cells were fixed with 1% paraformaldehyde PBS and incubated with anti-CXCR4 mAb. Cell were stained with FITC-conjugated secondary antibody and analyzed by flow cytometry.

Results

SDF-1α/CXCL12 induces tyrosine phosphorylation of Dok-1 and the association of Dok-1 with RasGAP, Nck, and Crk-L

Dok-1 is activated by different proteins, such as CD2.[21] To characterize signaling pathways activated by SDF-1α/CXCL12, we used the Jurkat T-cell line, which expresses the SDF-1α/CXCL12 receptor CXCR4. Jurkat cells were stimulated with 100 ng/mL SDF-1α/CXCL12 or control medium for 5 minutes. Cell lysates were subjected to anti–Dok-1 immunoprecipitation and to immunoblotting with antiphosphotyrosine antibody (Figure 1A). SDF-1α/CXCL12 stimulated the tyrosine phosphorylation of Dok-1. Nck is a ubiquitously expressed protein composed entirely of a single SH2 and 3 SH3 domains that fit into the adaptor class of

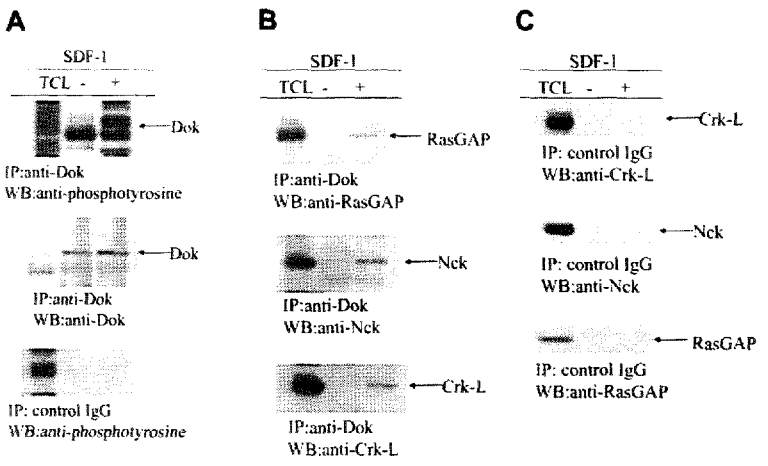

Figure 1. Dok-1 is tyrosine phosphorylated and associates with RasGAP, Nck, and Crk-L after SDF-1α/CXCL12 stimulation. (A) Jurkat cells were left unstimulated (−) or stimulated with SDF-1α/CXCL12 (100 ng/mL) for 5 minutes. Total cell lysates (TCLs) were immunoprecipitated with anti–Dok-1 Ab. Immunoprecipitates (IPs) were immunoblotted with antiphosphotyrosine antibody (upper panel) or anti–Dok-1 Ab (middle panel). As control, IPs were made with control IgG, and immunoblotting was performed with antiphosphotyrosine antibody (lower panel). (B) Immunoprecipitates were immunoblotted with anti-RasGAP, Nck, and Crk-L antibodies. (C) As a control for panel B, IPs with control IgG Ab were immunoblotted with anti-RasGAP, anti-Nck, or anti–Crk-L Abs. (A-C) Results are representative of at least 3 experiments. WB indicates Western blot.

signaling molecules.[22] Crk-L is in the family of Crk adaptor proteins and was discovered in the form of an oncogene carried by 2 sarcoma-inducing retroviruses.[23,24] Crk-L and Crk play a role in the signaling pathways of the T-cell receptor.[25,26] Dok-1 associates with RasGAP and the adaptor proteins Nck and Crk-L after stimulation.[27,28] To determine whether SDF-1α/CXCL12 induces the association of such molecules, coimmunoprecipitation experiments were performed. SDF-1α/CXCL12 triggering induced significant association of Dok-1 with RasGAP, Nck, and Crk-L (Figure 1B). Tyrosine phosphorylation of SDF-1/CXCL12–stimulated cells was not seen when control immunoglobulin G (IgG) was used for immunoprecipitation (Figure 1A, lower panel), and neither CrK-L, NcK, nor RasGAP was detected in control IgG immunoprecipitates (Figure 1C).

SDF-1α/CXCL12–induced Dok-1 tyrosine phosphorylation depends on Src kinase activity

Dok-1 protein is phosphorylated by a wide range of PTKs, and Src family kinases are involved in SDF-1α/CXCL12 signaling.[29] We tested the potential relationships of Src to Dok-1 for SDF-1/CXCL12 signaling by using the specific Src kinase inhibitor, PP2. Jurkat cells were pretreated with 10 μM PP2 for 30 minutes and then were stimulated with SDF-1α/CXCL12. Pretreatment of Jurkat cells with PP2 completely blocked Dok-1 phosphorylation (Figure 2A). PP2 was not toxic to Jurkat cells, as assessed by trypan blue exclusion and cell numbers (data not shown). Using GST fusion proteins, we found that Dok-1 directly binds to the src kinase family members, Fyn and Lck, after SDF-1α/CXCL12 stimulation but does not bind without SDF-1/CXCL12 treatment (Figure 2B). Lck regulates T-cell surface receptors, such as CD2 and CD4.[30,31] We used J.CaM1.6 cells, a derivative of Jurkat cells that are defective in Lck, to determine whether Lck played a role in the activation of Dok-1. Dok-1 phosphorylation was completely blocked in J.CaM1.6 cells (Figure 2C), but not in J.CaM1.6 cells engineered to express Lck (Figure 2D), in response to SDF-1α/CXCL12 (Figure 2C), suggesting that Lck is involved in the regulation of Dok-1 phosphorylation in J.CaM1.6 cells in response to SDF-1α/CXCL12. Cell surface expression of CXCR4 was not different between J.CaM1.6 cells and the parental Jurkat cells (Figure 2E), demonstrating that differences between the 2 cell lines were not attributed to surface expression of CXCR4.

SDF-1α/CXCL12 induces tyrosine phosphorylation of Pyk2, and Pyk2 association with Zap-70 and Vav

Pyk2 is expressed mainly in the central nervous system and in cells derived from hematopoietic lineages. Pyk2 is activated by a variety

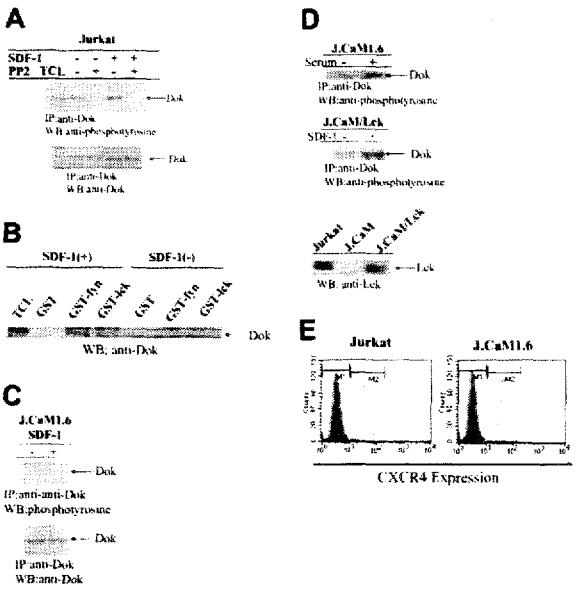

Figure 2. Dok-1 phosphorylation in response to SDF-1α/CXCL12 is blocked by src kinase inhibitor PP2, and Dok-1 is not phosphorylated in the Lck-deficient T-cell line J.CaM1.6. (A) Jurkat cells were pretreated with src kinase inhibitor PP2 (10 μM) for 30 minutes and were left unstimulated or stimulated with SDF-1α/CXCL12 at 100 ng/mL for 5 minutes. Cell lysates were immunoprecipitated with anti–Dok-1 Ab and were immunoblotted with antiphosphotyrosine (top panel) or anti–Dok-1 Ab (bottom panel). (B) Cells were stimulated with or without SDF-1, and cell lysates were incubated with agarose-conjugated GST, GST-fyn, or GST-lck and immunoblotted with anti-Dok Ab. (C) Total cell lysates from J.CaM1.6 cells were immunoprecipitated with anti–Dok-1 Ab and then immunoblotted with antiphosphotyrosine (top panel) or anti–Dok-1 Ab (bottom panel). (D) J.CaM1.6 cells were unstimulated or stimulated with serum. Cell lysates were incubated with anti–Dok Ab and were immunoblotted with antiphosphotyrosine Ab (top panel). J.CaM1.6 cells were unstimulated or stimulated with SDF-1. Cell lysates were incubated with anti-Dok Ab and immunoblotted with antiphosphotyrosine Ab (middle panel). Cell lysates of Jurkat, J.CaM1.6, and J.CaM/Lck were immunoblotted with anti-Lck Ab (bottom panel). (E) CXCR4 expression on Jurkat and J.CaM1.6 cells. Cells were fixed with 1% paraformaldehyde PBS. Cells were incubated with anti-CXCR4 mAb or normal mouse IgG and were stained with FITC-conjugated secondary Ab and analyzed by flow cytometry. (A-E) Results in each panel are representative of at least 3 experiments each.

of extracellular signals that elevate intracellular calcium concentration and by stress signals.[13,16] Phosphorylation of Pyk2 leads to the recruitment of src family kinases and activation of ERKs.[13,15] We evaluated a role for Pyk2 in SDF-1α/CXCL12 signaling. Pyk2 was tyrosine phosphorylated after SDF-1α/CXCL12 stimulation, without an effect on the total amount of Pyk2 (Figure 3A). Vav is a hematopoietic cell-specific guanine nucleotide exchange factor for small guanosine triphosphate (GT)–binding proteins.[32] Zap-70 is a PTK that associates with the ζ subunit of the TCR. Zap-70 is tyrosine phosphorylated after TCR stimulation.[33,34] As seen in Figure 3B, tyrosine-phosphorylated Pyk2 associates with Vav and Zap-70 after SDF-1α/CXCL12 stimulation.

SDF-1α/CXCL12 induces RasGAP association with Pyk2

RasGAP is an essential component of Ras-activated signaling pathways and down-regulates Ras activity. The association of RasGAP with Pyk2 was enhanced after SDF-1α stimulation (Figure 4). This suggests that RasGAP association with Pyk2 is involved in SDF-1α/CXCL12 signaling.

Overexpression of Dok-1 interferes with cell migration of CXCR4-expressing NIH3T3 and Baf3 cells and regulates MAPK activity in NIH3T3 cells

We demonstrated that Dok-1 associates with the adaptor proteins Nck and Crk-L (Figure 1B). Because Nck and Crk-L are involved in cell migration to SDF-1α/CXCL12,[35,36] we studied whether overexpression of Dok-1 influenced chemotaxis of CXCR4-expressing NIH3T3 and Baf3 cells in response to SDF-1α/CXCL12. Dok-1 cDNA was transfected to NIH3T3 cells expressing human CXCR4. Surface CXCR4 expression levels were not different between the parental CXCR4-expressing NIH3T3 cells

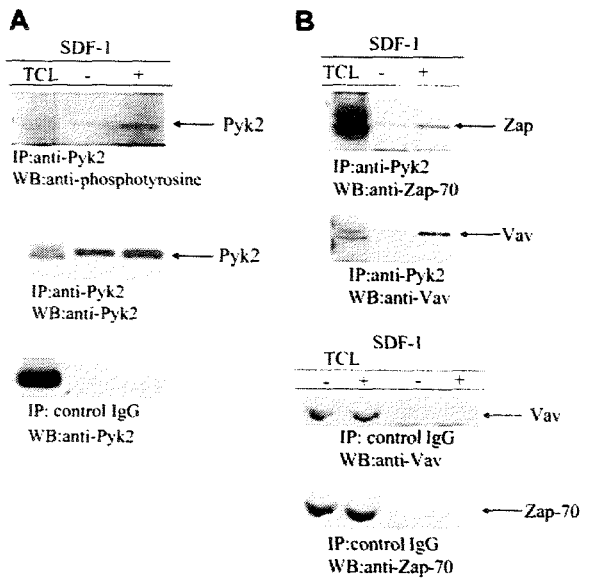

Figure 3. Pyk2 is tyrosine phosphorylated and associates with Zap-70 and Vav in Jurkat cells in response to SDF-1α/CXCL12. Cells were treated without and with SDF-1/CXCL12. (A) Pyk2 was immunoprecipitated from cell lysates of nonstimulated or SDF-1α/CXCL12–stimulated cells and was analyzed by Western blotting with antiphosphotyrosine (bottom panel) and Pyk2 (middle panel). As a control, control IgG–immunoprecipitated lysates were immunoblotted with anti-PyK2 Ab (bottom panel). (B) Anti-PyK2 (top two panels) or control IgG (bottom two panels) immunoprecipitates were immunoblotted with anti–Zap-70 or Vav Ab. (A-B) Results are representative of at least 3 experiments.

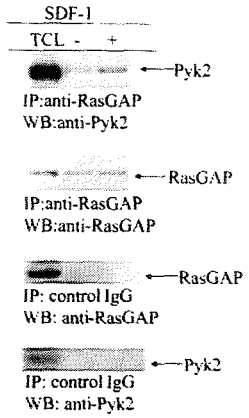

Figure 4. SDF-1α/CXCL12 induces RasGAP association with Pyk2 in Jurkat cells. RasGAP immunoprecipitates were analyzed by Western blotting with anti-Pyk2 or anti-RasGAP Ab. Shown are results of 1 of 3 representative experiments. IP controls for RasGAP and PyK2 are shown in the bottom two panels. The total amount of PyK2 did not change after treatment with SDF-1, similar to the results noted in Figure 3A.

transfected with empty vector and their dok-1 cDNA–transfected counterparts, as determined by flow cytometry and Western blot analysis (Figure 5A-B). Dok-1 overexpressing NIH3T3 cells were significantly decreased in response to SDF-1α/CXCL12–induced chemotaxis compared with empty vector–transfected NIH3T3 cells (Figure 5Ci). Baf3 cells and Baf3 cells overexpressing Dok-1 express similar levels of CXCR4 (data not shown). As seen in Figure 5Cii, Baf3 cells overexpressing Dok-1 were significantly suppressed in their chemotactic response to SDF-1/CXCL12. Dok-1 is considered a negative regulator of cell proliferation and Ras/MAPK signaling pathways.[10] To evaluate Dok-1 regulation of MAPK activity after SDF-1α/CXCL12 signaling, we used Dok-1–overexpressing NIH3T3 cells (Figure 5D-E). Dok-overexpressing NIH3T3 cells manifested reduced MAPK activity (Figure 5D) and decreased phosphorylation of Erk1 (Figure 5E) in response to SDF-1α/CXCL12 compared with mock-transfected cells. This suggests that Dok-1 plays a role in SDF-1α/CXCL12–induced chemotaxis and regulation of MAPK activity.

To determine the relevance and importance of Dok-1 in SDF-1/CXCL12–induced chemotaxis, we evaluated the chemotactic responses of T-lymphocyte subsets from the spleens of Dok-$1^{-/-}$ and Dok-$1^{+/+}$ mice[19] to graded amounts of SDF-1/CXCL12. As shown in Figure 6, total T cells, $CD4^+$ T cells, and $CD8^+$ T cells from the spleens of Dok-$1^{-/-}$ mice were enhanced in their chemotactic response to SDF-1/CXCL12; maximum enhancement occurred for Dok-$1^{-/-}$ T cells at a concentration of SDF-1/CXCL12 that maximally stimulated chemotaxis for Dok-$1^{+/+}$ T cells. Chemotaxis of Dok-$1^{-/-}$ and Dok-$1^{+/+}$ T cells to SDF-1CXCL12 was blocked by placing SDF-1/CXCL12 in the upper chamber or in both the upper and the lower chambers, demonstrating that the effects seen (migration to the lower chamber) were caused by chemotaxis and not by chemokinesis. Differences in chemotactic responses of Dok-$1^{-/-}$ and Dok-$1^{+/+}$ T cells to SDF-1/CXCL12 were not caused by differences in levels of expression of CXCR4 (Figure 6B). These results demonstrate that Dok-1 negatively regulates primary T-cell chemotaxis to SDF-1/CXCL12. Along with the data shown (Figure 5A, Ci-ii), Dok-1 may also negatively regulate the migration of other cell types to SDF-1/CXCL12.

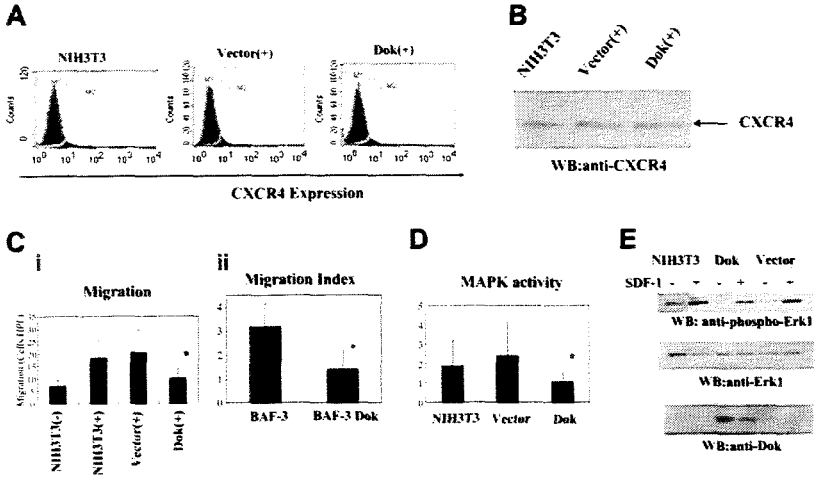

Figure 5. Influence of Dok-1 overexpression on SDF-1α/CXCL12–induced chemotaxis and activation of MAPK activity. (A) CXCR4 expression on NIH3T3 cells transfected with GFP-tagged full-length Dok-1 or with empty vector. Dok or vector-transfected NIH3T3 cells were incubated with anti-CXCR4 Ab or normal mouse IgG, stained with FITC-conjugated secondary Ab, and analyzed by flow cytometry. (B) CXCR4 protein from cell lysates of Dok or vector-transfected cells as assessed after immunoblotting with anti-CXCR4 Ab. (C) Chemotaxis in response to SDF-1α/CXCL12. (Ci) NIH3T3 cells were transfected with GFP-tagged full-length Dok-1 or with empty vector. Cell migration was analyzed in 48-well chemotaxis chambers. After sorting GFP$^+$ cells, 8000 cells were placed in the upper chambers. Three to 4 hours later, cells were stained using the DiffQuik kit, and the migrating cells were counted under high-power fields (× 400). Data represent the arithmetic mean ± SEM of 4 experiments. $^*P < .05$ compared with control vector. (Cii) Baf3 cells were transfected with full-length Dok-1. Cell migration was analyzed with chemotaxis chambers. Cells (2×10^5) input cells were placed in the upper chamber, and migrated cells were counted by fluorescence-activated cell sorter (FACS). Data represent the arithmetic mean ± SEM of 3 experiments. (D) MAPK activity. NIH3T3 cells were transfected with expression vector encoding Dok-1 or empty vector. Cells were stimulated with or without SDF-1α/CXCL12. Cells were fixed and stained with phospho-ERK1 Ab. MAPK activity was analyzed by flow cytometry. Data represent the arithmetic mean ± SEM of 5 experiments. $^*P < .05$ compared with control vector. (E) Phosphorylation of ERK-1. Dok or vector-transfected NIH3T3 cells were stimulated with SDF-1/CXCL12. Cell lysates were immunoblotted with anti-phospho Erk-1 Ab, Erk-1 Ab, or Dok Ab. Data represent results of 1 of 3 similar experiments.

Discussion

Chemokines belong to a large family of chemoattractant molecules and have been implicated in a number of different functions mediated through chemokine receptors. SDF-1α/CXCL12 plays a role in regulating the migration and homing of hematopoietic cells and is a highly efficient chemotactic factor for T cells. Several studies have evaluated the intracellular molecules involved in SDF-1α/CXCL12–induced chemotaxis of cells. In T cells, SDF-1α/CXCL12 stimulation results in activation of the Janus kinase/signal transduction and activation of transcription (Jak/STAT) pathways.[34] Phosphatidylinositol 3-kinase (PI3-K), Crk-associated substrate (p130Cas), focal adhesion kinase (FAK), and protein kinase C (PKC) are activated by SDF-1α/CXCL12,[35] but the signaling mechanisms involved are not yet fully determined. Our present report implicates the docking protein, Dok-1, as a mediator of SDF-1α/CXCL12–induced migration of T cells and associated intracellular signals; Dok-1 links with downstream effectors of SDF-1α/CXCL12/CXCR4 signaling. Dok-1 has typical features of

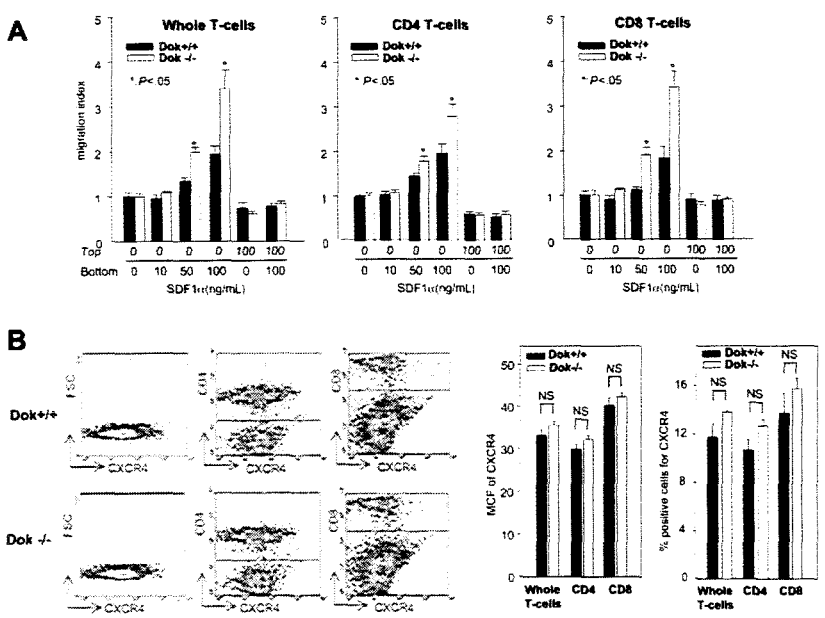

Figure 6. Migration to SDF-1α and CXCR expression of splenic T cells from control or Dok$^{-/-}$ mice. Half a million purified T cells from Dok$^{-/-}$ or control (Dok$^{+/+}$) mice were subjected to migration assay in a positive gradient of escalating doses of recombinant murine (rm) SDF-1α and a negative gradient and zero gradient of 100ng/mL of SDF-1α. After 4-hour migration, cells were enumerated by flow cytometry. (A) Input cells and migrated cells were stained with anti-CD4 and anti-CD8 antibodies to determine the numbers of CD4 and CD8 cells migrated. Migration index of whole, CD4, and CD8 cells are shown. Data are expressed as mean ± SEM from 6 mice of each group for CD4 cells (2 experiments with 3 mice each) and 3 mice of each group for whole or CD8 migration ($^*P < .05$ compared with control cells. (B) Isolated T cells were stained with anti-CXCR4 and anti-CD4 or anti-CD8 antibodies. (left) Result of 1 representative experiment. (right) Percentage of positive cells and mean channel fluorescence (MCF) for CXCR4. Data are mean ± SEM of 3 mice per group for 1 experiment. NS indicates not significant.

multiadaptor proteins, such as a membrane localization sequence (PH domain), receptor interaction domain (PTB domain), and several putative binding sites for downstream substrates (phosphotyrosine and PXXP elements). Dok-1 was identified as a tyrosine-phosphorylated protein of 62-kDa associated with p120RasGAP in fibroblasts transfected with v-src.[6] Dok-1 is phosphorylated by several receptor tyrosine kinases and is regulated by tyrosine kinase. Src family kinases, such as Src, Fyn, and Lck, regulate Dok-1 phosphorylation.[21] Lck is required for CD2-mediated phosphorylation of Dok-1. We have shown that Dok-1 tyrosine phosphorylation is completely blocked by use of the specific src kinase inhibitor PP2, implicating a reliance of Dok-1 on src family kinases (Figure 2A). We also found that Dok-1 phosphorylation was completely blocked after SDF-1α/CXCL12 stimulation in the Lck-deficient T-cell line J.CaM1.6 (Figure 2C), but not in J.CaM1.6 cells engineered to express LcK (Figure 2D), demonstrating that Lck regulates Dok-1 phosphorylation in this T-cell line.

Coimmunoprecipitation studies demonstrated that tyrosine-phosphorylated Dok-1 binds directly to RasGAP, Nck, and Crk-L. We had previously reported Nck involvement in SDF-1α/CXCL12 signaling and chemotaxis in Jurkat cells,[37] thereby implicating RasGAP, Nck, and CrK-L in SDF-1α/CXCL12–induced cell chemotaxis. To study the role of Dok-1 regulation of cell migration and MAPK activity in response to SDF-1α/CXCL12, Dok-1 cDNA was transfected into NIH3T3 cells expressing human CXCR4 and Baf3, which express CXCR4. Dok-1–transfected NIH3T3 and Baf3 cells were significantly less responsive to SDF-1α/CXCL12-induced chemotaxis than empty vector–transfected cells, directly demonstrating Dok-1 as one of the intracellular molecules involved in SDF-1α/CXCL12–induced migration. Analysis of Dok-1 knockout mice reveals that Dok-1 is a negative regulator of cell proliferation.[10] Cells derived from Dok-1 knockout mice hyperproliferate in response to a number of cytokines and growth factors. Moreover, we found that total T cells, as well as $CD4^+$ T cells and $CD8^+$ T cells, from the spleens of Dok-$1^{-/-}$ mice were enhanced in response to SDF-1/CXCL12–induced chemotaxis compared with Dok-$1^{+/+}$ T cells (Figure 6). Dok-1 negatively regulates MAPK activity in T cells. We also found that Dok-1 regulates MAPK activity in response to SDF-1α/CXCL12 signaling (Figure 5D-E).

Pyk2 is a non–receptor tyrosine kinase belonging to the focal adhesion kinase family. Pyk2 interacts with several signaling intermediates. Pyk2 has no SH2 or SH3 domains, but it is proposed that proline-rich stretches in the C-terminus act as ligands for SH3 domain–containing signaling proteins. Pyk2 is constitutively expressed in human T cells and is rapidly phosphorylated on the activation of TCR. This is associated with its increased association with Src and Grb2.[17,18] We found that Pyk2 is tyrosine phosphorylated after SDF-1α/CXCL12 stimulation in Jurkat cells. Moreover, the present data also show that Pyk2 associates with Zap-70 and Vav. Pyk2 has been shown to participate in the activation of MAPKs. RasGAP is implicated as a negative regulator of ras because it is capable of stimulating the intrinsic GTPase-inactive guanosine diphosphate (GDP)–bound form of the molecule. Interestingly, Pyk2 can bind to RasGAP after SDF-1α/CXCL12 stimulation. Thus, Pyk2 also appears to play a role in SDF-1α/CXCL12 signaling and perhaps in the regulation of MAPK activity.

In summary, we have demonstrated that SDF-1α/CXCL12 action leading to Dok-1 activation is dependent on src kinases and on Pyk2. Several signaling pathways are induced by SDF-1α/CXCL12. These signaling pathways are regulated by positive and negative regulators. Dok-1 appears to play a negative role in SDF-1α/CXCL12 signaling and chemotaxis, and Pyk2 may play a positive role.

References

1. Bleul CC, Fuhlbrigge RC, Casasnovas JM, Aiuti A, Springer TA. A highly efficacious lymphocyte chemoattractant, stromal cell–derived factor 1 (SDF-1). J Exp Med. 1996;184:1101-1109.
2. Broxmeyer HE, Kim CH. Regulation of hematopoiesis in a sea of chemokine family members with a plethora of redundant activities. Exp Hematol. 1999;27:1113-1123.
3. Bleul CC, Farzan M, Choe H, et al. The lymphocyte chemoattractant SDF-1 is a ligand for LESTR/fusin and blocks HIV-1 entry. Nature. 1996;382:829-833.
4. Nagasawa T, Hirota S, Tachibana K, et al. Defects of B-cell lymphopoiesis and bone-marrow myelopoiesis in mice lacking the CXC chemokine PBSF/SDF-1. Nature. 1996;382:635-638.
5. Zou YR, Kottmann AH, Kuroda M, Taniuchi I, Littman DR. Function of the chemokine receptor CXCR4 in haematopoiesis and in cerebellar development. Nature. 1998;393:595-599.
6. Ellis C, Moran M, McCormick F, Pawson T. Phosphorylation of GAP and GAP-associated proteins by transforming and mitogenic tyrosine kinases. Nature. 1990;343:377-381.
7. Yamanashi Y, Baltimore D. Identification of the Abl- and rasGAP-associated 62 kDa protein as a docking protein, Dok. Cell. 1997;88:205-211.
8. Kaplan DR, Morrison DK, Wong G, McCormick F, Williams LT. PDGF beta-receptor stimulates tyrosine phosphorylation of GAP and association of GAP with a signaling complex. Cell. 1990;61:125-133.
9. Hosomi Y, Shii K, Ogawa W, et al. Characterization of a 60-kilodalton substrate of the insulin receptor kinase. J Biol Chem. 1994;269:11498-11502.
10. Yamanashi Y, Tamura T, Kanamori T, et al. Role of the rasGAP-associated docking protein p62(dok) in negative regulation of B cell receptor-mediated signaling. Genes Dev. 2000;14:11-16.
11. Boguski MS, McCormick F. Proteins regulating Ras and its relatives. Nature. 1993;366:643-654.
12. Lev S, Moreno H, Martinez R, et al. Protein tyrosine kinase PYK2 involved in Ca(2+)-induced regulation of ion channel and MAP kinase functions. Nature. 1995;376:737-745.
13. Scheffzek K, Ahmadian MR, Wittinghofer A. GTPase-activating proteins: helping hands to complement an active site. Trends Biochem Sci. 1998;23:257-262.
14. Sasaki H, Nagura K, Ishino M, Tobioka H, Kotani K, Sasaki T. Cloning and characterization of cell adhesion kinase beta, a novel protein-tyrosine kinase of the focal adhesion kinase subfamily. J Biol Chem. 1995;270:21206-21219.
15. Avraham S, London R, Fu Y, et al. Identification and characterization of a novel related adhesion focal tyrosine kinase (RAFTK) from megakaryocytes and brain. J Biol Chem. 1995;270:27742-27751.
16. Yu H, Li X, Marchetto GS, et al. Activation of a novel calcium-dependent protein-tyrosine kinase: correlation with c-Jun N-terminal kinase but not mitogen-activated protein kinase activation. J Biol Chem. 1996;271:29993-29998.
17. Wange RL, Samelson LE. Complex complexes: signaling at the TCR. Immunity. 1996;5:197-205.
18. Valitutti S, Dessing M, Aktories K, Gallati H, Lanzavecchia A. Sustained signaling leading to T cell activation results from prolonged T cell receptor occupancy: role of T cell actin cytoskeleton. J Exp Med. 1995;181:577-584.
19. Di Cristofano A, Niki M, Zhao M, et al. p62(dok), a negative regulator of Ras and mitogen-activated protein kinase (MAPK) activity, opposes leukemogenesis by p210(bcr-abl). J Exp Med. 2001;194:274-284.
20. Kim CH, Broxmeyer HE. In vitro behavior of hematopoietic progenitor cells under the influence of chemoattractants: stromal cell–derived factor-1, steel factor, and the bone marrow environment. Blood. 1998;91:100-110.
21. Nemorin JG, Duplay P. Evidence that Lck-mediated phosphorylation of p56dok and p62dok may play a role in CD2 signaling. J Biol Chem. 2000;275:14590-14597.
22. Lehmann JM, Riethmuller G, Johnson JP. Nck, a melanoma cDNA encoding a cytoplasmic protein consisting of the src homology units SH2 and SH3 [abstract]. Nucleic Acids Res. 1990;18:1048.
23. Mayer BJ, Hamaguchi M, Hanafusa H. A novel viral oncogene with structural similarity to phospholipase C. Nature. 1988;332:272-275.
24. Tsuchie H, Chang CH, Yoshida M, Vogt PK. A newly isolated avian sarcoma virus, ASV-1, carries the crk oncogene. Oncogene. 1989;4:1281-1284.
25. Boussiotis VA, Freeman GJ, Berezovskaya A, Barber DL, Nadler LM. Maintenance of human T cell anergy: blocking of IL-2 gene transcription by activated Rap1. Science. 1997;278:124-128.
26. Reedquist KA, Bos JL. Costimulation through CD28 suppresses T cell receptor-dependent activation of the Ras-like small GTPase Rap1 in human T lymphocytes. J Biol Chem. 1998;273:4944-4949.
27. Holland SJ, Gale NW, Gish GD, et al. Juxtamembrane tyrosine residues couple the Eph family

receptor EphB2/Nuk to specific SH2 domain proteins in neuronal cells. EMBO J. 1997;16:3877-3888.

28. Songyang Z, Shoelson SE, Chaudhuri M, et al. SH2 domains recognize specific phosphopeptide sequences. Cell. 1993;72:767-778.
29. Okabe S, Fukuda S, Broxmeyer HE. Src kinase, but not the src kinase family member p56lck, mediates stromal cell–derived factor 1α/CXCL12 induced chemotaxis of a T cell line. J Hematother Stem Cell Res. 2002;11:932-938.
30. Veillette A, Bookman MA, Horak EM, Bolen JB. The CD4 and CD8 T cell surface antigens are associated with the internal membrane tyrosine-protein kinase p56lck. Cell. 1988;55:301-308.
31. Carmo AM, Mason DW, Beyers AD. Physical association of the cytoplasmic domain of CD2 with the tyrosine kinases p56lck and p59fyn. Eur J Immunol. 1993;23:2196-2201.
32. Bustelo XR. Regulatory and signaling properties of the Vav family. Mol Cell Biol. 2000;20:1461-1477.
33. Arpaia E, Shahar M, Dadi H, Cohen A, Roifman CM. Defective T cell receptor signaling and CD8+ thymic selection in humans lacking zap-70 kinase. Cell. 1994;76:947-958.
34. Zhang XF, Wang JF, Matczak E, Proper JA, Groopman JE. Janus kinase 2 is involved in stromal cell–derived factor-1α–induced tyrosine phosphorylation of focal adhesion proteins and migration of hematopoietic progenitor cells. Blood. 2001;97: 3342-3348.
35. Lupher ML Jr, Reedquist KA, Miyake S, Langdon WY, Band H. A novel phosphotyrosine-binding domain in the N-terminal transforming region of Cbl interacts directly and selectively with ZAP-70 in T cells. J Biol Chem. 1996;271:24063-24068.
36. Wang JF, Park IW, Groopman JE. Stromal cell–derived factor-1α stimulates tyrosine phosphorylation of multiple focal adhesion proteins and induces migration of hematopoietic progenitor cells: roles of phosphoinositide-3 kinase and protein kinase C. Blood. 2000;95:2505-2513.
37. Okabe S, Fukuda S, Broxmeyer HE. Activation of Wiskott-Aldrich syndrome protein and its association with other proteins by stromal cell–derived factor-1α is associated with cell migration in a T-lymphocyte line. Exp Hematol. 2002;30:761-766.

A G-quadruplex-interactive agent, telomestatin (SOT-095), induces telomere shortening with apoptosis and enhances chemosensitivity in acute myeloid leukemia

M. SUMI[1], T. TAUCHI[1], G. SASHIDA[1], A. NAKAJIMA[1], A. GOTOH[1], K. SHIN-YA[3], J.H. OHYASHIKI[2] and K. OHYASHIKI[1]

[1]First Department of Internal Medicine, [2]Intractable Immune-Disease Research Center, Tokyo Medical University, Shinjuku-ku, Tokyo 160-0023; [3]Institute of Molecular and Cellular Biosciences, The University of Tokyo, Bunkyo-ku, Tokyo 113-0032, Japan

Received December 29, 2003; Accepted February 27, 2004

Abstract. Telomerase, the ribonucleoprotein enzyme maintaining the telomeres of eukaryotic chromosomes, is up-regulated in the vast majority of human neoplasias but not in normal somatic tissues. Therefore, the telomerase complex represents a promising universal therapeutic target in cancer. Telomeric G-rich single-stranded DNA can adopt *in vitro* an intramolecular quadruplex structure, which has been shown to inhibit telomerase activity. We examined G-quadruplex interactive agent, telomestatin (SOT-095), for its ability to inhibit the proliferation of human leukemia cells, including freshly obtained leukemia cells. Telomere length was determined by either the terminal restriction fragment method or flow-FISH, and apoptosis was assessed by flow cytometry. Moreover, chemosensitivity was examined in telomestatin-treated U937 cells before ultimate telomere shortening. Treatment with telomestatin reproducibly inhibited telomerase activity in U937 and NB4 cells followed by telomere shortening. Enhanced chemosensitivity toward daunorubicin and cytosine-arabinoside was observed in telomestatin-treated U937 cells, before ultimate telomere shortening. Telomere shortening associated with apoptosis by telomestatin was evident in some freshly obtained leukemia cells from acute myeloid leukemia patients, regardless of sub-types of AML and post-myelodysplasia AML. These results suggest that disruption of telomere maintenance by telomestatin limits the cellular lifespan of AML cells, as well. However, in a minority of AML patients apoptosis was not evident, thus indicating that resistant mechanism might exist in some freshly obtained AML cells. Therefore, further investigation of telomestatin as a therapeutic agent is warranted.

Correspondence to: Dr Tetsuzo Tauchi, First Department of Internal Medicine, Tokyo Medical University, 6-7-1 Nishishinjuku, Shinjuku-ku, Tokyo 160-0023, Japan
E-mail: ohyashik@tokyo-med.ac.jprr.iij4u.or.jp

Key words: G-quadruplex, telomerase inhibition, acute myeloid leukemia, apoptosis, chemosensitivity

Introduction

The reactivation of telomerase activity in most cancer cells supports the concept that telomerase is a relevant target in oncology, and telomerase inhibitors have been proposed as new potential anticancer agents (1,2). Several genetic experiments using a dominant-negative form of human telomerase have demonstrated that telomerase inhibition can result in telomere shortening followed by proliferation arrest and cell death by apoptosis (3-5). One effective strategy for the design of telomerase inhibitors targets telomerase indirectly, via the telomeric substrate, and aims to block the interaction between the enzyme and the telomere (1). At the extreme 3'-termini of telomeres there are regions of single-stranded DNA, formed because of a limitation of the DNA polymerization mechanism known as the end-replication problem (6,7). These regions have a G-rich, single-stranded structure assembled around a core stack of guanines arranged in almost-planar, hydrogen-bonded tetrads. Ionic conditions that favor quadruplex formation have been shown to inhibit telomerase (8), and small molecules that stabilize or promote the formation of quadruplexes also show inhibitory activity (9-12). Thus, quadruplex DNA presents a target of considerable importance in DNA-directed drug design.

Telomestatin (SOT-095) is a natural product isolated from *Streptomyces anulatus* 3533-SV4 and has been shown to stabilize G-quadruplex structures (13). The structural similarity between telomestatin and the G-quadruplex suggests that telomere disruption may be caused by the ability of telomestatin to either facilitate the formation of G-quadruplex structures or trap out G-quadruplexes that have already formed, thereby sequestering single-stranded d[T2AG3]n primer molecules (14). We have reported that telomestatin induced down-regulation of telomerase activity followed by ultimate telomere shortening and apoptosis in Philadelphia-positive leukemic cells (15). Moreover, it is demonstrated that telomestatin induced the activation of ATM and Chk2, and subsequently increased the expression of $p21^{CIP1}$ and $p27^{KIP1}$,

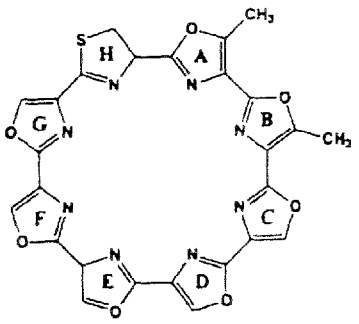

Figure 1. Structure of telomestatin. Telomestatin is a natural product isolated from *Streptomyses anulants* 3533-SV4. The structure of telomestatin is very similar to that of the G-tetrad.

indicating that telomere dysfunction induced by telomestatin activates the ATM-dependent DNA damage response (16). Therefore, telomestatin may effect acute myeloid leukemia, including freshly obtained leukemia cells, and we assessed modulation of anti-leukemic agents that may induce DNA damage.

Materials and methods

Cells and agents. U937 cells and NB4 cells were obtained from the American Type Culture Collection (Rockville, MD). These cell lines were cultured in McCoy's 5A modified medium (Life Technology Inc.) supplemented with 10% fetal calf serum (Hyclone Laboratories, Logan, UT). Daunorubicin (DNR), cytosine arabinoside (Ara-C), etoposide (VP-16), vincristine (VCR), 6-mercaptopurine (6-MP), and methotrexate (MTX) were purchased from Sigma (St. Louis, MO). Telomestatin (SOT-095) has been described previously (Fig. 1), (13,14).

Telomerase assay and telomere measurement. Telomerase activity was measured by a telomere repeat amplification

Table I. Characteristics of acute myeloid leukemia cells treated with telomestatin *in vitro*.

UPN	Age/ gender	Diagnosis	WBC	Blast (%)	Karyotypes	Surface markers (CD)	Source of *in vitro* study	Percentage of APO 2.7		Telomere length (kb)	
								Before	After	Before	After
1	54/F	AML-M1-relapse	9,000	31	46,XX	13/33/117/34/71/DR/7	PB	1.58	28.30	9.3	6.1
2	59/M	AML-M1	16,100	75	33-39,XY,-10,-11,-12,-16,-17,-18,-19,-20	13/33	BM	4.19	21.70	5.7	5.3
3	61/M	AML-M2	24,600	97	46/XY/46/XY add(21)(q22)	13/33/117/34/56/DR/7	PB	4.26	76.70	ND	ND
4	52/M	AML-M3	20,100	16 (66)	46,XY,t(15;17)(q22;q21),46,XY,idem,add(7)(q31)	13/14/38/33	PB	18.20	28.80	19.8	16.7
5	47/M	AML-M4Eo	31,600	82	46,XY/45,X,-Y,inv(16)(p13q22)/46,X,-Y,idem,+21	13/33/34/117/DR	BM	12.10	17	8.9	5.9
6	53/M	Post-MDS AML	3,000	16	47,XY,-7,-18,+3mar	13/33/117/34/71/DR	BM	2.71	17.90	5.5	5.2
7	74/M	Post-MDS AML	6,800	48	46,XY	13/15/117/34/56/71/DR	BM	4.87	12.20	ND	ND
8	63/M	Post-MDS AML	9,600	83	46,XY	15/33/64/65/11b/56/DR	PB	10.20	62	13.5	5.8
9	70/M	Post-MDS AML	5,400	48	46,XY,der(7)t(1;7)(q10;p10)/47,XY,idem,+8/48,XY,idem,+8,+8	13/33/94/117/34/DR	BM	4.04	4.50	ND	ND

Gender: M, male; F, female. Source of *in vitro* study: PB, peripheral blood; BM, bone marrow. Telomere length: before, before telomestatin treatment; after, after telomestatin treatment.

protocol (TRAP) assay using a TRAPeze telomerase detection kit (Oncor, Gaithersburg, MD) (17,18). To measure terminal restriction fragment (TRF) length, genomic DNA was digested with restriction enzymes (HinfI or RsaI) and assessed using the Telo TTAGGG telomere length assay kit (Roche Molecular Biochemicals, Mannheim, Germany). Smears of the developed films were captured on an Image Master (Pharmacia Biotech, Uppsala, Sweden), and defined the TRF in each sample as the peak intensity of telomeric length, in kilobases (kb), by densitometry (19).

We employed flow-FISH, since this method is very useful for analysis of clinical samples with small numbers of cells. Telomere length measurements of primary leukemia cells were performed by flow-FISH, as previously described (21,22). Briefly, cells were washed in phosphate-buffered saline and were divided equally into two 1.5-ml tubes. After centrifugation cells were resuspended in the hybridization mixture (10^5 cells/μl) with 0.3 μg/ml telomere-specific FITC-conjugated PNA probe (Dako, Denmark). The cells were washed three times and resuspended in DNA-staining solution with propidium iodide and RNase A. The samples were then analyzed by flow cytometry (Epics XL Beckman Coulter, Fullerton, CA). Daily shifts in the linearity of the flow cytometer and fluctuations in the laser intensity and alignment were compensated for by using FITC-labeled fluorescent beads (Quantum-24 Premixed; Flow Cytometry Standards, San Juan, Puerto Rico). To analyze the day-to-day variation in flow-FISH results, aliquots of cells derived from a primary calf thymus cells were analyzed in each experiment. Formula: telomere length = 4.551+0.077 (AU/telomere fluorescence of referential calf thymus cell), AU = telomere fluorescence of sample with probe - telomere fluorescence of sample without probe.

Apoptosis assay. The incidence of apoptosis was determined by flow cytometric analysis with FITC-conjugated APO2.7 monoclonal antibody (clone 2.7), which was raised against the 38-kDa mitochondrial membrane protein (7A6 antigen) and is expressed by cells undergoing apoptosis (15).

Primary leukemic cells. Primary leukemic blasts were freshly isolated from 9 patients with acute myeloid leukemia after obtaining informed consent from patients who had been referred to the Tokyo Medical University Hospital. The nine leukemia patients consisted of two AML-M1, one AML-M2, one AML-M3, one AML-M4Eo, and four post-myelodysplastic AML (post-MDS AML) (Table I). Leukemic enriched fraction was obtained by Ficoll-Hypaque gradient method and analyzed for apoptosis test and telomere length was measured using the flow-FISH.

Statistical analysis. Comparisons between groups were analyzed by Student's t-test. Values of $p<0.05$ were considered to indicate statistical significance. Statistical tests were performed with the Microsoft Word Excel software package (Brain Power, Calabashes, CA) on a Macintosh personal computer.

Results

Effects of telomestatin on telomerase activity and telomere length in a human leukemia cell line. To study the effects of telomestatin on telomerase activity, we first cultured U937 cells with various concentrations of telomestatin for 48 h. Telomestatin appears to be a potent telomerase inhibitor, with 50% inhibition at ~2 μM (Fig. 2A). To examine the long-term effects of telomestatin on U937 cells and NB4 cells, it was necessary to identify the drug concentration window in which telomerase could be inhibited without extensive inhibition of cell proliferation. Addition of 2 μM of telomestatin had no effect on short-term cell viability or proliferation, as determined in a 7-day cytotoxicity assay. Therefore, we used 2 μM as the treatment concentration in long-term cultivation experiments.

In the presence of telomestatin, the TRF length of U937 cells shortened progressively from 9.5 to 5.0 kb at population

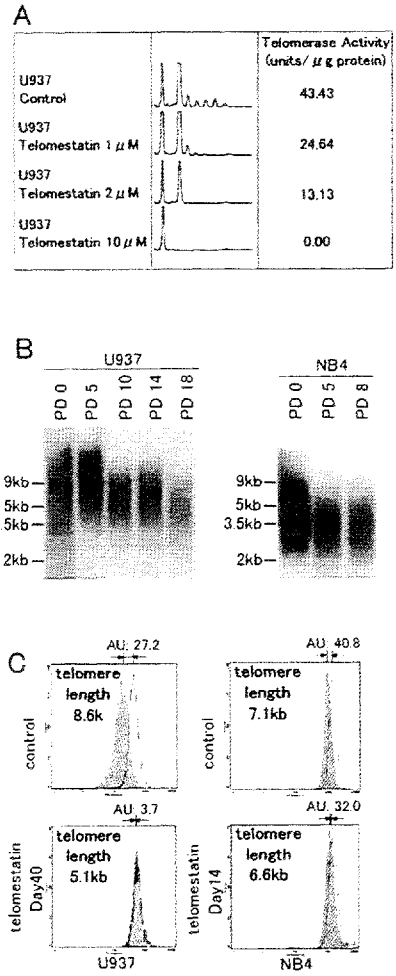

Figure 2. Effects of telomestatin on telomerase activity and telomere length in leukemia cells. (A), Effect of telomestatin on telomerase activity in U937 cells. U937 cells were incubated with the indicated concentrations of telomestatin for 48 h, then telomerase activity was examined by a TRAP assay. Telomerase activity was suppressed by telomestatin in a dose-dependent manner. (B), Telomere length in U937 cells and NB4 cells was assessed for telomere restriction fragment size by Southern blot analysis with a telomeric probe. In both myeloid leukemia cell lines, telomere length was progressively shortened after telomestatin treatment at indicated population doubling (PD). (C), U937 cells and NB4 cells were cultured with or without 2 μM of telomestatin for the number of days indicated, and telomere length was determined by flow-FISH analysis. This indicates, in combination with (B), that flow-FISH method is reproducible to determine telomere length in leukemia cells.

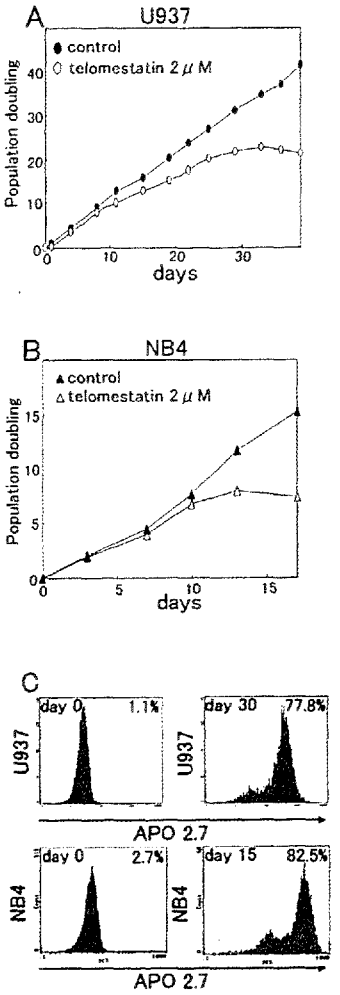

Figure 3. Effects of telomestatin on cell proliferation. U937 cells (A) and NB4 cells (B) were plated in 24-well plates in the presence of 2 μM of telomestatin in 0.1% methanol. Control cells were treated with 0.1% methanol. Cultures were replated every 3 or 4 days to maintain log-phase growth and to calculate the growth rate. (C), U937 cells and NB4 cells were cultured with 2 μM of telomestatin for the number of days indicated. The incidence of apoptosis was determined by flow cytometric analysis with FITC-conjugated APO 2.7 mAb (clone 2.7). Most leukemia cells showed apoptosis after incubation of telomestatin: 77.8% of telomestatin treated U937 cells at 30 day and 82.5% of telomestatin treated NB4 cells at 15 day showed apoptosis.

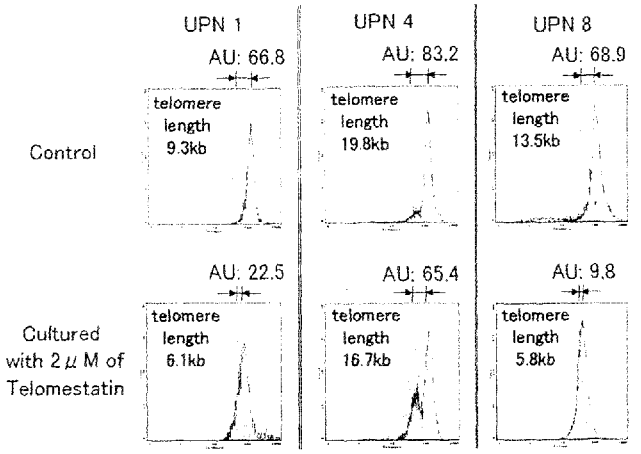

Figure 4. Effects of telomestatin on telomere reduction in freshly obtained human acute myeloid leukemia cells. Primary leukemia cells were incubated for 10 days in the absence or presence of 2 μM telomestatin. The telomere length was determined by flow-FISH. The telomere lengths were assessed using the formula (Materials and methods). Representative cases are shown.

doubling (PD) 18, and TRF length in telomestatin-treated NB4 cells also shortened from 4.8 to 3.5 kb (Fig. 2B). The telomere shortening after cultivation of 2 μM telomestatin was also confirmed by flow-FISH analysis using the PNA probe (Fig. 2C). This clearly indicates that telomere length, as well as TRF length that includes sub-telomeric region, actually shortened at the time of appropriate PD in telomestatin-treated myeloid leukemia cells (U937 and NB4 lines).

Effects of telomestatin on cell proliferation and apoptosis. The growth kinetics of telomestatin-treated cells initially did not differ from those of untreated control cells, regardless of the cell line used. After 30 days (around PD 20), telomestatin-treated U937 cells showed an almost complete inhibition of proliferation (Fig. 3A), whereas telomestatin-treated NB4 cells ceased to proliferate after 13 days (around PD 8) (Fig. 3B) with distinctive morphological features associated with apoptosis. The percentage of apoptosis increased in U937 cells from 1.1 to 77.8% at day 30 and in NB4 cells from 2.7 to 82.5% at day 15 (Fig. 3C). These results demonstrate that telomestatin inhibits telomerase activity in myeloid leukemia cells, resulting in telomere shortening, which may lead to subsequent induction of apoptosis.

Telomere shortening and induction of apoptosis in primary acute leukemia cells after exposure to telomestatin. Freshly isolated leukemic cells (>85% blast cells) were incubated in suspension cultures in the absence or presence of 2 μM of telomestatin for 10 days, and the occurrence of apoptosis was examined by APO2.7 antibody testing; in some case, telomere length was determined by flow-FISH, as well. Eight of 9 samples showed an increasing frequency of apoptosis after treatment of telomestatin, and 6 of them (UPN 1, 2, 3, 6, 7, and 8) showed more than two-holds increase in the percentage of apoptosis (Table I). Representatively, addition of 2 μM of telomestatin increased the incidence of apoptosis (from 1.58 to 28.3%), accompanied by telomere shortening (from 9.3 to 6.1 kb) in UPN 1. The same effect was also reproducible in UPN 8: apoptosis occurred (from 10.2 to 62.0%) accompanied by telomere shortening (from 13.5 to 5.8 kb) after 10 days incubation with telomestatin (Fig. 4). These results suggest that telomere shortening by telomestatin induces apoptosis in some primary blast cells from acute leukemia, regardless of sub-types of AML. This effect seemed not to be restricted in de novo AML but post-MDS AML.

However, the frequency of apoptosis was <20% in some cases (4/9 patients). One patient with post-MDS AML (UPN 9) did not show an increase in percentages of APO 2.7-positive cells after telomestatin treatment (from 4.04 to 4.5%). One possibility might be due to the timing of determination of apoptosis in this study. Another plausible explanation for limiting effect in inducing apoptosis might be due to alternative mechanism of telomere elongation (ALT) (22,23). Leukemic

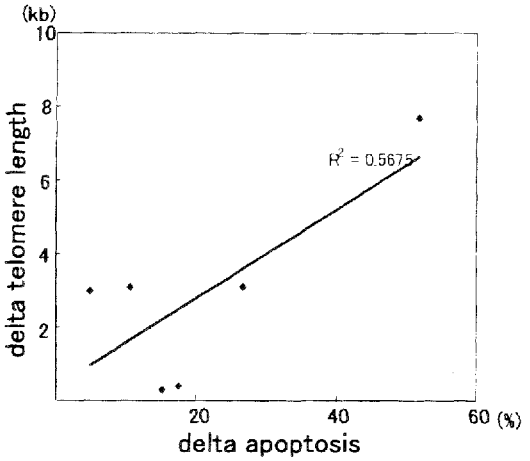

Figure 5. Correlation between delta-telomere and delta-apoptosis in freshly obtained acute myeloid leukemia cells with 10-days culture of 2 μM telomestatin. Vertical axis shows delta-telomere length = telomere length with telomestatin-telomere length without telomestatin (kb). Horizontal axis shows delta-apoptosis = apoptosis with telomestatin-apoptosis without telomestatin (%).

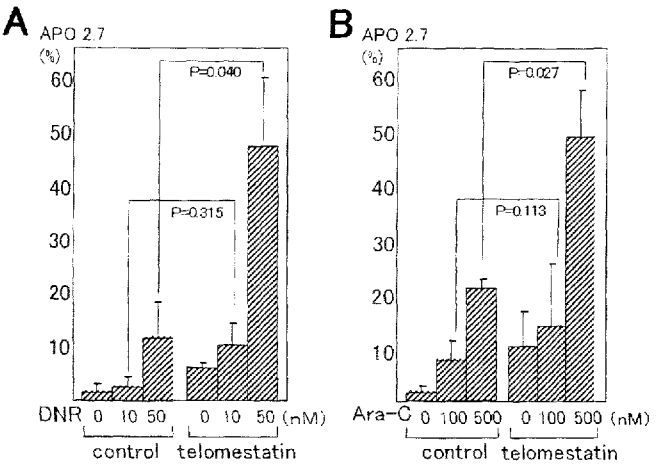

Figure 6. Enhancement of apoptosis from DNR or AraC treatment in telomestatin-treated U937 cells. U937 cells cultured with 2 μM telomestatin at PD 10 were incubated with the indicated concentrations of DNR (A) or AraC (B) for 48h. The incidence of apoptosis was determined by flow cytometric analysis with APO 2.7 mAb. Similar results were obtained in two independent experiments.

cells from UPN 4 did not show remarkable shortening of telomere length after telomestatin treatment (from 19.8 to 16.7 kb) with a limited effect for apoptosis (from 18.2 to 28.8%) (Fig. 4). Though there seems to be variety between telomere reduction and the frequency of apoptosis after telomestatin treatment *in vitro* in leukemia cells obtained from AML patients, there was a correlation between reduction of the length of telomeres and the frequency of apoptosis (Fig. 5). This indicates that apoptosis in AML cells by telomestatin might be related to the reduction of telomere length.

Enhanced apoptosis in response to chemotherapeutic agents in telomestatin-treated U937 cells. We next assessed the effects of telomerase inhibition in modulating responses to chemotherapeutic agents at relatively early-passage telomestatin-treated U937 cells (PD10), since early-passage telomestatin-treated U937 cells showed partial induction of apoptosis (<10%) and limited cessation of cellular proliferation (Fig. 3A), without telomerase activity. Subsequently, the telomestatin-treated U937 cells were incubated with the chemotherapeutic agents for 48 h. The U937 cells without pre-treatment with telomestatin showed approximately 11% apoptosis after 50 nM DNR treatment, while 49% telomestatin treated cells showed apoptosis after the same concentration of DNR (11.4±6.4% vs. 48.9±12.3%; p=0.04). This tendency was also evident after 500 nM Ara-C treatment (20.7±1.6% vs. 48.8±8.4%; p=0.027). The lower concentrations of DNR (10 nM) or Ara-C (100 nM) treated U937 cells showed an enhanced induction of apoptosis as well, but not significant (p=0.315 and p=0.113, respectively) (Fig. 6). By contrast, enhanced chemosensitivity was not observed in cells exposed to VCR, VP-16, 6-MP, or MTX (data not shown). This enhanced sensitivity regarding apoptosis to some classes of chemotherapeutic agents indicates that there is cytotoxic synergy between telomere dysfunction and these agents.

Discussion

Telomere shortening is thought to be important in the regulation of cellular senescence and up-regulation of telomerase activity may be critical in the development of neoplastic cells. One prediction of this model is that specific inhibition for telomerase function alters the growth properties relating to telomere dysfunction of neoplastic cells and thus may be candidates of a new strategy for universal anti-neoplastic therapy (1). Genetic experiments using a dominant-negative form of human telomerase demonstrated that telomerase inhibition can result in telomere shortening followed by proliferation arrest and cell death by apoptosis (3-5). Several other strategies to inhibit telomerase activity have been reported so far: a recent study described N3'>P5' thio-phosphoramidate oligonucleotides as telomerase template antagonists (GRN163), which should display improved clinical efficacy (25). These approaches selectively act on neoplastic cells with high telomerase activity and are suitable for 'target therapy' for neoplasia. However, this method limits the proportion of the completely telomerase-negative clone that sometimes exists in telomerase-positive population or tumors with telomerase-independent telomere elongation (22,23). Moreover, telomerase activity in human acute leukemia is generally not high when compared to solid tumors (26,28), thus indicating that target therapy against telomerase in human acute leukemia might be limited to monotherapy.

In the current study, we tested the therapeutic possibility of telomestatin for acute myeloid leukemia. Telomestatin induces telomere shortening, as well as down-regulation of telomerase activity, and apoptosis in human myeloid leukemia cell lines. Since telomestatin selectively stabilizes intramolecular G-quadruplexes, including telomere sequences [T_2AG_3], telomestatin might also exert an effect directly and is expected to induce more rapid onset of telomere shortening and cellular senescence. Since effectiveness of target therapy against the telomerase actually depends on the 'end-

replication problem', cells in the arrest phase may escape from the attack. Moreover, action of telomestatin may be independent of the levels of telomerase activity, thus human acute leukemia might be suitable for target therapy with telomestatin. We also observed that telomere shortening by telomestatin also induced apoptosis in some primary blast cells freshly obtained from AML patients. However, some fresh AML cells with shortened telomeres exceptionally showed limited effect in inducing apoptosis after telomestatin treatment. It should be clarified whether the determination timing of apoptosis in this study is enough to detect cellular senescence or the existence of abolish mechanism of telomestatin. Although we did not have a chance to measure telomerase activity in fresh AML cells in this study, telomestatin might affect growth and survival of acute leukemia cells with or without high levels of telomerase activity.

G-quadruplex-forming sequences are also found in several transcriptional regulatory regions of important oncogenes, including c-*myc*, c-*myb*, c-*fos*, and c-*abl* (29). Because of the polypurine-polypyrimidine nature of these duplex sequences, which contain 4 or more runs of clusters of three or more guanines on the purine-rich strand, they often show a single-stranded character and hence are hypersensitive to nucleases. In the c-myc promoter, the purine- and pyrimidine-rich strands bind transcription factors [cellular nucleic-acid-binding protein (CNBP), and heterogeneous nuclear ribonuclear protein (hnRNP)] that are required for transcriptional activation (30). As these elements can also form G-quadruplex and I-motif structures, it is possible that the secondary DNA structures inactivate transcription, and their conversion to duplex regions is required for transcriptional activation (31). These issues indicate possible benefit to use telomestatin not only for the purpose of telomere-telomerase inhibitor but also transcriptional inhibitor of key gene(s) for proliferation of leukemic cells.

Our study using fresh AML cells demonstrated that reduction of telomere varied from 0.3 to 7.8 kb after only 10 days of culture with telomestatin. It is too early to induce telomere shortening only due to the 'end-replication problem' after shutting off telomerase activity. Telomere reduction usually takes place 100 bp around one cell cycle and 4-5 cell cycles during a 10 day-culture, thus several kb reductions of telomeres in our experiments using freshly obtained AML cells might be due to telomere-disruption mechanism by telomestatin. This supports the concept that telomestatin directly attacks telomeres and induces telomere shortening, resulting in apoptosis of acute leukemia cells. Thus, telomestatin might have multi-function for not only a telomerase-telomere maintenance mechanism but also regulation mechanism of certain oncogene(s).

Telomerase-specific inhibitors usually show certain lag-time to cellular senescence until telomere shortening. Therefore, we assessed chemosensitivity before ultimate telomere shortening in acute myeloid leukemia cells, and confirmed that DNR and Ara-C could be beneficial in combination with telomestatin in inducing cell death. Lee *et al* reported that neoplastic cells from telomerase RNA null mice (mTERC-/-) showed enhanced chemosensitivity to DNR or related double-strand DNA break (DSB)-inducing agents (32). Telomere dysfunction, rather than telomerase inhibition, is proposed to be the principal determinant governing chemosensitivity specifically to DSB-inducing agents (32). We also reported that telomestatin induced the activation of ATM and Chk2, and subsequently increased the expression of $p21^{CIP1}$ and $p27^{KIP1}$, indicating that telomere dysfunction induced by telomestatin activates the ATM-dependent DNA damage response (16). However, we were unable to detect enhanced induction of apoptosis by VP-16, VCR, 6-MP, or MTX in telomestatin-treated U937 cells. VP-16 is a topoisomerase II inhibitor and induces DSBs, as does DNR. Therefore, it will be important to resolve the question of why these two different kinds of DSB-inducing agent have different effects on chemosensitivity in telomestatin-treated cells. Although the exact mechanism of the enhanced induction of apoptosis in telomestatin-treated cells requires further elucidation, telomerase inhibition and telomere dysfunction has previously been shown to enhance the chemosensitivity of tumor cells to DNA-damaging agents (33).

Acknowledgements

This work was supported by grants from the Ministry of Education, Science and Culture of Japan (to T.T.); the Tokyo Medical University high-tech research center for intractable immune diseases and the Ministry of Education, Culture, Sports, Science, and Technology of Japan (to K.O.).

References

1. Bearss DJ, Hurley LH and Von Hoff DD: Telomere maintenance mechanisms as a target for drug development. Oncogene 19: 6632-6641, 2000.
2. White LK, Wright WE and Shay JW: Telomerase inhibitors. Trends Biotech 19: 114-120, 2001.
3. Hahn WC, Stewart SA, Brooks MW, York SG, Eaton E, Kurachi A, Beijersbergen RL, Knoll JHM, Meyerson M and Weinberg RA: Inhibition of telomerase limits the growth of human cancer cells. Nat Med 5: 1164-1170, 1999.
4. Zhang X, Mar V, Zhou W, Harrington L and Robinson MO: Telomere shortening and apoptosis in telomerase-inhibited human tumor cells. Genes Dev 13: 2388-2399, 1999.
5. Tauchi T, Nakajima A, Sashida G, Shimamoto T, Ohyashiki JH, Abe K, Yamamoto K and Ohyashiki K: Inhibition of human telomerase enhances the effect of the tyrosine kinase inhibitor, imatinib, in BCR-ABL-positive leukemia cells. Clin Cancer Res 8: 3341-3347, 2002.
6. Watson JD: Origin of concatameric T7 DNA. Nature 239: 197-201, 1972.
7. Olovnikov AM: A theory of marginotomy. J Ther Biol 41: 181-190, 1973.
8. Zahler AM, Williamson JR, Cech TR and Prescott DM: Inhibition of telomerase by G-quartet DNA structures. Nature 350: 718-720, 1991.
9. Sun D, Thompson B, Cathers BE, Salazar M, Kerwin SM, Trent JO, Jenkins TC, Neidle S and Hurley LH: Inhibition of human telomerase by a G-quadruplex-interactive compound. J Med Chem 40: 2113-2116, 1997.
10. Wheelhouse RT, Sun D, Han H, Han FX and Hurley LH: Cationic porphyrins as telomerase inhibitors: interaction of tetra (N-methyl-4-pyridyl) porphyrin with quadruplex DNA. J Am Chem Soc 120: 3261-3262, 1998.
11. Perry PJ and Jenkins TC: Recent advances in the development of telomerase inhibitors for the treatment of cancer. Exp Opin Invest Drugs 8: 1981-2008, 1999.
12. Izbicka E, Wheelhouse RT, Raymond E, Davidson KK, Lawrence RA, Sun D, Windle BE and Hurley LH: Effects of cationic porphyrins as G-quadruplex interactive agents in human tumor cells. Cancer Res 59: 639-644, 1999.
13. Shin-ya K, Wierzba K, Matsuo K, Ohtani T, Yamada Y, Furihata K, Hayakawa Y and Seto H: Telomestatin, a novel telomerase inhibitor from *Streptomyces anulatus*. J Am Chem Soc 123: 1262-126, 2001.

14. Kim MY, Vankayalapati H, Shin-Ya K, Wierzba K and Hurley LH: Telomestatin, a potent telomerase inhibitor that interacts quite specifically with the human telomeric intramolecular G-quadruplex. J Am Chem Soc 124: 2098-2099, 2002.
15. Nakajima A, Tauchi T, Sashida G, Sumi M, Abe K, Yamamoto K, Ohyashiki JH and Ohyashiki K: Telomerase inhibition enhannces apoptosis in human acute leukemia cells: possibility of anti-telomerase therapy. Leukemia 17: 560-567, 2003.
16. Tauchi T, Shin-ya K, Sashida G, Sumi M, Nakajima A, Simamoto T, Ohyashiki JH and Ohyashiki K: Activity of novel G-quadruplex-interactive telomerase inhibitor, telomestatin (SOT-095), against human leukemia cells: involvement of ATM-dependent DNA damage response pathways. Oncogene 14: 5338-5347, 2003.
17. Piatyszeck MA, Kim MY, Weinrich SL, Hiyama K, Hiyama E, Wright WE and Shay JW: Detection of telomerase activity in human cells and tumors by a telomeric repeat amplification protocol (TRAP). Method Cell Sci 17: 1-15, 1995.
18. Ohyashiki JH, Ohyashiki K, Toyama K and Shay JW: A non-radioactive, fluorescence-based telomeric repeat amplification protocol to detect and quantitate telomerase activity. Trends Genet 12: 395-396, 1996.
19. Iwama H, Ohyashiki K, Ohyashiki JH, Hayashi S, Yahata N, Ando K, Toyama K, Hoshika A, Takasaki M, Mori M and Shay JW: Telomeric length and telomerase activity vary with age in peripheral blood cells obtained from normal individuals. Hum Genet 102: 397-402, 1998.
20. Rufer N, Brummendorf TH, Kolvraa S, Bischoff C, Christensen K, Wadsworth L, Schulzer M and Lansdorp PM: Telomere fluorescence measurements in granulocytes and T lymphocyte subsets point to a high turnover of hematopoietic stem cells and memory T cells in early childhood. J Exp Med: 157-167, 1999.
21. Misawa M, Tauchi T, Sashida G, Nakajima A, Abe K, Ohyashiki JH and Ohyashiki K: Inhibition of human telomerase enhances the effect of chemotherapeutic agents in lung cancer cells. Int J Oncol 21: 1087-1092, 2002.
22. Bryan TM, Englezou A, Gupta J, Bacchetti S and Reddel RR: Telomere elongation in immortal human cells without detectable telomerase activity. EMBO J 14: 4240-4248, 1995.
23. Dunham MA, Neumann AA, Fasching CL and Reddel RR: Telomere maintenance by recombination in human cells. Nat Genet 26: 447-450, 2001.
24. Delhommeau F, Thierry A, Feneux D, Lauret E, Leclercq E, Coutier MH, Stainteny F and Vainchenker W: Telomere dysfunction and telomerase reactivation in human leukemia cell lines after telomerase inhibition by the expression of a dominant-negative hTERT mutant. Oncogene 21: 8262-8271, 2002.
25. Asai A, Oshima Y, Yamamoto Y, Uochi T, Kusakawa H, Akinaga S, Yamashita Y, Pongracz K, Pruzan R, Wunder E, Piatyszek M, Li S, Chin AC, Harley CB and Gryaznov S: A novel telomerase template antagonist (GRN163) as a potential anticancer agent. Cancer Res 63: 3931-3939, 2003.
26. Ohyashiki JH, Ohyashiki K, Iwama H, Hayashi S, Toyama K and Shay JW: Clinical implications telomerase activity levels in acute leukemia. Clin Cancer Res 3: 619-624, 1997.
27. Engelhardt M, MacKenzie K, Drullinsky P, Silver RT and Moore MA: Telomerase activity and telomere length in acute and chronic leukemia, pre- and post-*ex vivo* culture. Cancer Res 60: 610-617, 2000.
28. Ohyashiki JH, Sashida G, Tauchi T and Ohyashiki K: Telomeres and telomerase in hematopoietic neoplasia. Oncogene 21: 680-687, 2002.
29. Hurley LH: DNA and its associated processes as targets for cancer therapy. Nat Rev Cancer 2: 188-200, 2002.
30. Simonsson T, Pecinka P and Kubista M: DNA tetraplex formation in the control region of c-myc. Nucleic Acids Res 26: 1167-1172, 1998.
31. Siddiqui-Jain A, Grand CL, Bearss DJ and Hurley LH: Direct evidence for a G-quadruplex in a promoter region and its targeting with a small molecule to repress c-MYC transcription. Proc Natl Acad Sci USA 99: 11593-11598, 2002.
32. Lee KH, Rudolph KL, Ju YJ, Greenberg RA, Cannizzaro L, Chin L, Weiler SR and DePinho RA: Telomere dysfunction alters the chemotherapeutic profile of transformed cells. Proc Natl Acad Sci USA 98: 3381-3386, 2001.
33. Stewart SA, Hahn WC, O'Connor BF, Banner EN, Lundberg AS, Modha P, Mizuno H, Brooks MW, Fleming M, Ziomonjic DB, Popescu NC and Weinberg RA: Telomerase contributes to tumorigenesis by a telomere length-independent mechanism. Proc Natl Acad Sci USA 99: 12606-12611, 2002.

GENES, CHROMOSOMES & CANCER 42:269–279 (2005)

Identification of a SRC-Like Tyrosine Kinase Gene, *FRK*, Fused with *ETV6* in a Patient with Acute Myelogenous Leukemia Carrying a t(6;12)(q21;p13) Translocation

Noriko Hosoya,[1] Ying Qiao,[1] Akira Hangaishi,[1] Lili Wang,[1] Yasuhito Nannya,[1] Masashi Sanada,[1] Mineo Kurokawa,[1] Shigeru Chiba,[1,2] Hisamaru Hirai,[1,2] and Seishi Ogawa[1,3]*

[1]Department of Hematology and Oncology, Graduate School of Medicine, University of Tokyo, Tokyo, Japan
[2]Department of Cell Therapy and Transplantation Medicine, University of Tokyo Hospital, University of Tokyo, Tokyo, Japan
[3]Department of Regeneration Medicine for Hematopoiesis, Graduate School of Medicine, University of Tokyo, Tokyo, Japan

The SRC family of kinases is rarely mutated in primary human tumors. We report the identification of a SRC-like tyrosine kinase gene, *FRK* (Fyn-related kinase), fused with *ETV6* in a patient with acute myelogenous leukemia carrying t(6;12)(q21;p13). Both reciprocal fusion transcripts, *ETV6/FRK* and *FRK/ETV6*, were expressed. In *ETV6/FRK*, exon 4 of *ETV6* was fused in-frame to exon 3 of *FRK*, producing a chimeric protein consisting of the entire oligomerization domain of ETV6 and the kinase domain of FRK. The ETV6/FRK protein was shown to be constitutively autophosphorylated on its tyrosine residues. ETV6/FRK phosphorylated histones H2B and H4 in vitro to a greater extent than did FRK, suggesting it had elevated kinase activity. ETV6/FRK could transform both Ba/F3 cells and NIH3T3 cells, which depended on its kinase activity. Moreover, ETV6/FRK inhibited ETV6-mediated transcriptional repression in a dominant-negative manner. This report provides the first evidence that a SRC-like kinase gene, *FRK* fused with *ETV6*, could directly contribute to leukemogenesis by producing an oncoprotein, ETV6/FRK, with dual functions: constitutive activation of the ETV6/FRK tyrosine kinase and dominant-negative modulation of ETV6-mediated transcriptional repression.

INTRODUCTION

The *SRC* gene was the first protooncogene isolated as the cellular homologue of v-*SRC*, the retroviral transforming oncogene of avian Rous sarcoma virus (Brown and Cooper, 1996). Since then, it has become clear that *SRC* is the prototype for a family of genes that encode nonreceptor tyrosine kinases implicated in a variety of cellular processes, including cell growth, differentiation, and carcinogenesis. The SRC family of kinases shares common structures consisting of an N-terminal unique domain, SRC homology 3 (SH3) and SRC homology 2 (SH2) domains, a kinase domain, and a short C-terminal regulatory tail (Brown and Cooper, 1996). They are normally maintained in an inactive state through phosphorylation of a critical C-terminal tyrosine residue (Tyr 530 in human SRC, Tyr 527 in chicken SRC) by the C-terminal SRC kinase (Csk) (Brown and Cooper, 1996). The SH3 and SH2 domains also participate in this negative regulation through intramolecular interactions (Brown and Cooper, 1996; Schindler et al., 1999; Xu et al., 1999; Young et al., 2001).

The SRC and its family member kinases have long been postulated to participate in oncogenic processes. Activated variants of SRC family kinases, including the viral oncoprotein v-SRC, are capable of inducing malignant transformation in a variety of cell types (Parker et al., 1984; Cartwright et al., 1987). Activation of SRC-like kinases recently was described in *BCR-ABL1*-expressing acute lymphoblastic leukemia in mice (Hu et al., 2004). Elevated expression and/or activity of SRC have been documented in several types of primary human tumors (Bolen et al., 1987; Ottenhoff-Kalff et al., 1992; Talamonti et al., 1993). However, for many years, structural abnormalities of the SRC family of kinases have been detected rarely in primary human tumors. Although Irby et al. (1999)

Supported by: Research on Human Genome and Tissue Engineering, Health and Labour Sciences Research Grants, Ministry of Health, Labour and Welfare of Japan; Japan Society for the Promotion of Science; Grant number: KAKENHI 14570962.

*Correspondence to: Seishi Ogawa, Department of Hematology and Oncology, Department of Regeneration Medicine for Hematopoiesis, Graduate School of Medicine, University of Tokyo, 7-3-1, Hongo, Bunkyo-ku, Tokyo 113-8655, Japan.
E-mail: sogawa-tky@umin.ac.jp

Received 22 July 2004; Accepted 15 October 2004
DOI 10.1002/gcc.20147
Published online 20 December 2004 in Wiley InterScience (www.interscience.wiley.com).

reported that 12% of advanced human colon cancers had a truncating mutation at codon 531 of the *SRC* gene, determining the importance of this mutation in the generation of colorectal cancers remained elusive according to the negative results in subsequent reports (Daigo et al., 1999; Wang et al., 2000; Laghi et al., 2001). In primary hematopoietic malignancies, no studies have demonstrated structural abnormalities of the SRC family of kinases.

In this study, we performed molecular analysis of a t(6;12)(q21;p13) observed as the sole chromosomal abnormality in a case of acute myelogenous leukemia (AML) and identified a SRC-like tyrosine kinase gene, *FRK* (Fyn-related kinase or *Rak*), on 6q21 (Cance et al., 1994; Lee et al., 1994) that is fused with *ETV6* (also called *TEL*), a gene frequently involved in chromosomal translocations in a variety of human leukemias (Golub et al., 1997). We found that the resultant chimeric protein, ETV6/FRK, is a transforming oncoprotein with elevated kinase activity. We also demonstrated that ETV6/FRK inhibits ETV6-mediated transcriptional repression in a dominant-negative manner, indicating that ETV6/FRK is a unique oncoprotein with dual functions. This is the first report showing the involvement of a SRC-like kinase gene (*FRK*) in primary human cancers.

MATERIALS AND METHODS

Case History

The patient was a 69-year-old Japanese woman with AML-M4, carrying the translocation t(6;12)(q21;p13) as the sole chromosomal abnormality in 8 of 20 examined bone marrow metaphase cells. After obtaining informed consent, a sample of her bone marrow was taken for use in this study. The patient did not respond to chemotherapy and died 5 months later.

Fluorescence In Situ Hybridization Analysis

Fluorescence in situ hybridization (FISH) analysis was performed as previously described (Pinkel et al., 1986) with a panel of biotin- and digoxigenin-labeled cosmid probes that contained different exons of *ETV6*, kindly provided by Dr. Peter Marynen (University of Leuven, Leuven, Belgium). The order and the relative locations of cosmids are depicted in Figure 1A.

3′-Rapid Amplification of cDNA End

To do the 3′-rapid amplification of cDNA end (RACE), total RNA was isolated from the leukemic sample as described previously (Ogawa et al., 1996). First-strand cDNA was synthesized from 2.5 μg of total RNA using the primer R2N6 as described previously by Peeters et al. (1997). The first polymerase chain reaction (PCR) was performed with primers T4F1 and R2N6R1 (Peeters et al., 1997). Then, a diluted product of the first PCR, along with primers T4F2 and R2N6R2, was used for the second, nested PCR (Peeters et al., 1997). The nucleotide sequences of the primers used in this study and the conditions for PCR are listed in Table 1. The PCR products were subcloned into the pCR® 2.1-TOPO® vector using a TOPO TA Cloning® kit (Invitrogen, Tokyo, Japan) and subjected to DNA sequencing by use of a 3100 Applied Biosystems automated sequencer (Applied Biosystems, Chiba, Japan).

Reverse Transcriptase–PCR

For the reverse transcriptase-PCR (RT-PCR), 5 μg of the total RNA was transcribed to cDNA with 2 units of Moloney murine leukemia virus reverse-transcriptase (MMLV-RT, Stratagene, La Jolla, CA) using a random hexamer. One-tenth of the synthesized cDNA was directed to PCR analysis. Primers T4F2 and FRK1198R were used to confirm the *ETV6/FRK* transcripts. The primers for detecting the reciprocal *FRK/ETV6* transcripts were FRK451F and TEL723R. For amplification of the wild-type *ETV6* and *FRK* transcripts, primers T4F2 and TEL723R and primers FRK808F and FRK1198R, respectively, were used. All the sequences of the RT-PCR products were verified by direct sequencing.

Plasmid Construction

Full-length *ETV6* cDNA tagged with a FLAG sequence at the 5′ end, a gift from Dr. Kinuko Mitani (Dokkyo University School of Medicine, Tochigi, Japan), was subcloned into the expression plasmid pME18S-neo (Invitrogen, San Diego, CA). A FLAG-tagged full-length *FRK* cDNA was isolated by RT-PCR from total RNA obtained from human placenta using primers *Eco*RI-FLAG-FRK and FRK-*Not*I-2058R and was cloned into pME18S-neo. The pME18S-neo-FLAG-ETV6/FRK vector was generated by replacement of the *Cla*I-*Not*I fragment of the pME18S-neo-FLAG-ETV6 vector with the *Cla*I-*Not*I fragment of *ETV6/FRK*, which was obtained by RT-PCR from the patient's bone marrow using primers TEL-*Cla*I-F and FRK-*Not*I-2058R, with subsequent digestion with *Cla*I and *Not*I. To construct a kinase-inactive mutant of ETV6/FRK, designated ETV6/FRK(K262R), a point mutation corresponding

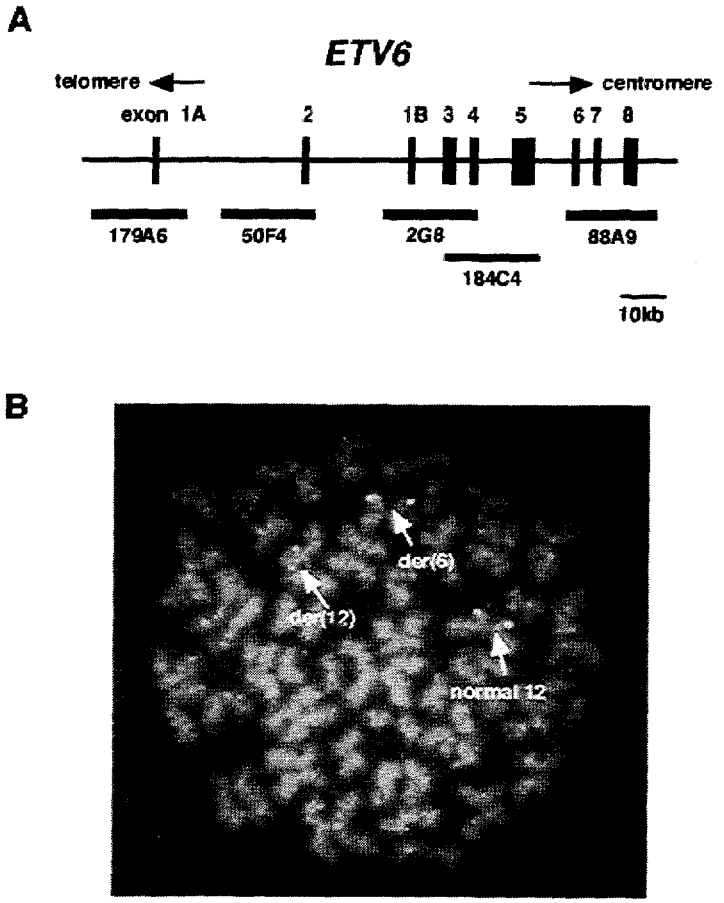

Figure 1. Analysis of breakpoint on chromosome 12. (A) A genomic map of *ETV6* and location of the cosmid probes used for FISH analysis. (B) FISH analysis of the patient's leukemic cells. The signals of the 2G8 probe (red) containing *ETV6* exons 1B, 3, and 4 are hybridized on the der(6) and on the normal 12p, whereas those of the 184C4 probe (green) containing *ETV6* exons 3–5 are found on the der(6), the der(12), and the normal 12p.

to a kinase-inactivating mutation in the ATP-binding site lysine residue (Lys262) of FRK was introduced into *ETV6/FRK* cDNA. A mutated fragment generated by PCR using the mutagenic primer FRK-K262R-*Bam*HI and the primer TEL-*Eco*RI-FLAG was spliced together with a C-terminal partial fragment of *FRK* into pME18S-neo. A FLAG-tagged full-length *FRK/ETV6* cDNA was constructed into the pME18S-neo vector by assembling partial fragments from *ETV6* and *FRK* and a fragment spanning the *FRK/ETV6* junction generated by RT-PCR using primers FRK451F and TEL723R. All the constructs were sequenced to confirm the fidelity of the sequence and conservation of the reading frame at the site of fusion.

Cell Lines, Transfection, and Cell Transformation Studies

For transient expression studies, 4×10^4 HeLa cells were seeded in each 60-mm dish and transfected with expression plasmid or plasmids 24 hr later by a lipofection method using Effectine™ Transfection Reagent (Qiagen, Hilden, Germany). Cells were incubated for 48 hr and harvested for analysis. NIH3T3 cells were transfected with expression plasmids, also using Effectine™, and selected in 400 μg/ml of G418 for 2 weeks. Ba/F3 clones stably expressing ETV6/FRK or other proteins were obtained by electroporation of each expression plasmid into Ba/F3 cells as previously described (Carroll et al., 1996) and subsequent isolation of individual G418-resistant subclones by limiting dilution. Expression of the transfected genes was evaluated by immunoblotting as previously described (Maki et al., 1999) using anti-FLAG-M2 monoclonal antibody (Sigma-Aldrich, St. Louis, MO). The soft-agar colony assay was performed as previously described (Kurokawa et al., 1996). After 21 days, all macroscopic colonies larger than 0.25 mm in diameter were counted. For growth curves, 2×10^4 G418-resistant Ba/F3 cells were washed 3 times with PBS and plated in IL-3-free medium on day 0, and viable cells were counted each day by trypan blue exclusion.

TABLE 1. Primers Used For 3'-RACE and (RT)-PCR Amplifications

Name	Sequence
R2N6	5'-CCAGTGAGCAGAGTGACGAGGACTCGAGCTCAAGC(N)6-3'
T4F1	5'-CATATTCTGAAGCAGAGGAAA-3'
R2N6R1	5'-CCAGTGAGCAGAGTGACG-3'
T4F2	5'-ACACAGCCGGAGGTCATACT-3'
R2N6R2	5'-GAGGACTCGAGCTCAAGC-3'
FRK1198R	5'-CTTCCCATACTTCGCAAAC-3'
FRK451F	5'-AGCAACATCTGTCAGAGGCT-3'
TEL723R	5'-GTAGGACTCCTGGTGGTTGTT-3'
FRK808F	5'-ATCGGAAGATCAGATGCAGAG-3'
*Eco*RI-FLAG-FRK	5'-GCGAATTCGTTGTGATGGGGGACTACAAGGACGAC GATGACAAGTCCGGGAGCAACATCTGTCAGAGGCT-3'
FRK-*Not*I-2058R	5'-ATTGCGGCCGCACTGATTGTGCAGTTGGTTGA-3'
TEL-*Cla*I-F	5'-CTTTCGCTATCGATCTCCTCA-3'
TEL-*Eco*RI-FLAG	5'-GCGAATTCGTTGTGATGGGGGACTACAAGGACGAC GATGACAAGTCCGGGTCTGAGACTCCTGCTCAGTG-3'
FRK-K262R-*Bam*HI	5'-TTGGATCCATTGAACCTGGTTTTAATGTTCTCACTG-3'

Thermal cycling profile was: 94°C for 2 min, followed by 35 cycles of 94°C for 1 min, 60°C for 1 min and 72°C for 2 min, with a final extension at 72°C for 10 min.

Immunoprecipitation, Immunoblotting, and Immune Complex Kinase Assay

Lysates were prepared by washing cells (1×10^6–1×10^7) with phosphate-buffered saline and then adding lysis buffer [10 mM Tris-HCl (pH 7.4), 150 mM NaCl, 1.0% NP-40, 1 mM EDTA, and 1 mM Na3VO4] containing 5 mM phenylmethyl-sulfonylfluoride and 1 μg/ml of aprotinin. After 10 min on ice, the samples were centrifuged at 12,000 g to remove insoluble particles. For immunoprecipitation, 1 mg of total cell lysate was incubated with anti-FLAG-M2 antibody for 1 hr at 4°C, after which 50 μl of Protein G-Sepharose beads (Amersham Biosciences, Uppsala, Sweden) was added. After rotating for 1 hr at 4°C, immunoprecipitates were washed 3 times and boiled in loading buffer for 5 min. Protein samples were separated on 6.5%–15% gradient SDS-polyacrylamide gels and transferred onto PVDF membranes (Millipore, Bedford, MA). Immunoblotting was performed as previously described (Maki et al., 1999) using either anti-FLAG-M2 antibody or antiphosphotyrosine monoclonal antibody 4G10 (Upstate Biotechnology Incorporated, Lake Placid, NY) as a primary antibody.

For the immune complex kinase assay, immunoprecipitates were washed 3 times and suspended in kinase buffer [40 mM HEPES (pH 7.4), 10 mM $MgCl_2$, 5 mM $MnCl_2$]. For determination of kinase activity, 2.5 μg of either histone H2B or histone H4 (Roche Diagnostics K. K., Tokyo, Japan) was added to each reaction. Kinase reactions were initiated by the addition of 10 μCi of [γ-^{32}P] ATP (3,000 Ci/mmol; Amersham Biosciences Corp., Piscataway, NJ) and incubated at 30°C for 15 min. Reactions were stopped by the addition of loading buffer and analyzed by SDS-PAGE and exposure to a film.

Luciferase Assay

For the luciferase assay, 4×10^4 HeLa cells were transfected with 1 μg of the reporter plasmid (EBS)3tkLuc (Waga et al., 2003), a kind gift of Dr. Kinuko Mitani, along with the indicated amounts of the expression vectors. The total amount of DNA in weight was adjusted to be equal by adding pME18S-neo plasmid. Luciferase activities were determined as described previously (Maki et al., 1999). All transfection experiments were performed in duplicate at least 3 times.

RESULTS

Identification of the Breakpoint on Chromosome 12

We performed FISH experiments using several probes from the *ETV6* locus, on 12p13 (Fig. 1A). The signals from the cosmids containing exons 1–4 (179A6, 50F4, and 2G8) were found on the der(6) (Fig. 1B), whereas the signals from the cosmid containing exons 3–5 (184C4) were split to the der(6) and the der(12) (Fig. 1B), suggesting that the breakpoint on 12p13 was localized to *ETV6* exons 4–5. The signals on the normal 12p were always observed with all the indicated cosmid probes of the *ETV6* locus, suggesting that the non-

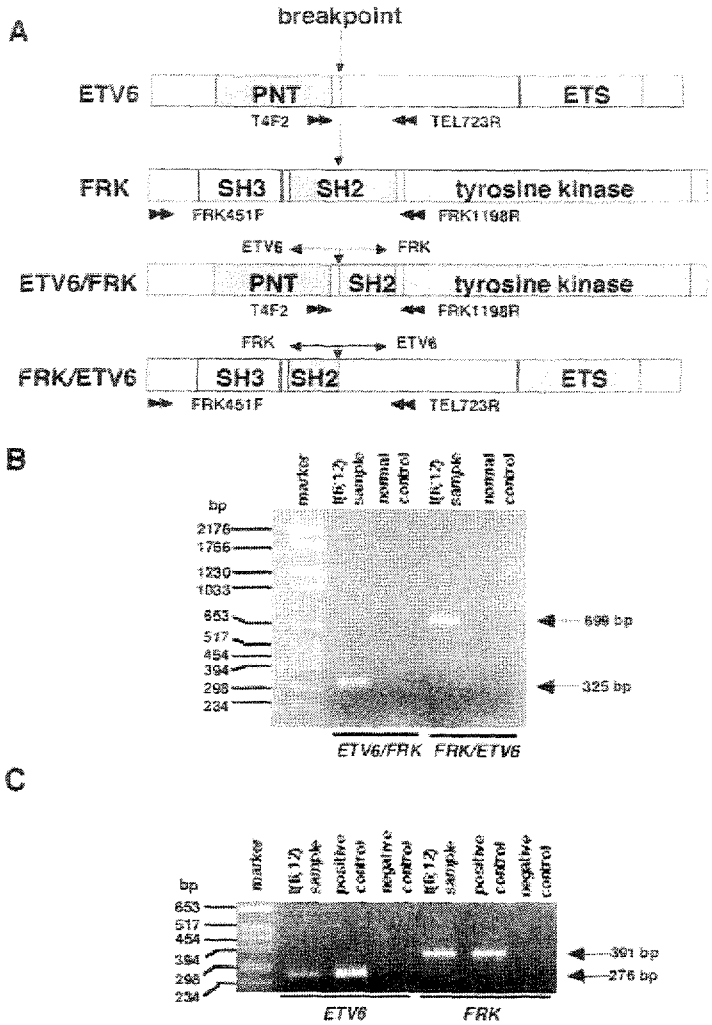

Figure 2. Identification of *ETV6/FRK* and *FRK/ETV6* fusion transcripts. (A) Schematic representation of wild-type *ETV6*, *FRK*, and the fusion transcripts. The breakpoints are indicated by vertical arrows. Horizontal arrows indicate the positions of RT-PCR primers (described in the Materials and Methods section). (B) Detection of *ETV6/FRK* as well as *FRK/ETV6* fusion transcripts by RT-PCR in the patient's leukemic sample. (C) Expression of *ETV6* and *FRK* in the patient's leukemic sample by RT-PCR.

translocated allele of *ETV6* was grossly intact with no large deletions.

Identification of the Fusion Partner of *ETV6*

To identify the unknown fusion partner of *ETV6*, 3′-RACE-PCR was performed. After two rounds of PCR, 3′-RACE-PCR products were successfully obtained. Sequencing analysis of the PCR products showed that exon 4 of *ETV6* was fused to exon 3 of *FRK* on 6q21, creating an *ETV6/FRK* fusion gene. The *FRK* gene encodes a SRC-like nonreceptor tyrosine kinase, consisting of the N-terminal SH3 and SH2 domains, the C-terminal kinase domain, and a short regulatory tail (Fig. 2A). The *ETV6/FRK* fusion gene produced a chimeric protein in which the entire pointed (PNT) oligomerization domain (also called helix–loop–helix domain) of ETV6 and the kinase domain of FRK were fused in-frame (Fig. 2A).

Detection of the *ETV6/FRK* and *FRK/ETV6* Fusion Transcripts

RT-PCR analysis was performed to confirm the fusion transcripts of the *ETV6* and *FRK* genes. Both reciprocal fusion transcripts, *ETV6/FRK* and *FRK/ETV6*, were specifically amplified from the leukemic sample but not from control bone marrow (Fig. 2B). Expression of wild-type *ETV6* and *FRK* also was detected in the leukemic sample (Fig. 2C). There were no mutations in the entire coding sequences of *ETV6*, *FRK*, *ETV6/FRK*, and *FRK/ETV6* (data not shown).